Geometric calibration of industrial robots using enhanced partial pose measurements and design of experiments

Yier Wu, Alexandr Klimchik, Stéphane Caro, Benoit Furet, Anatol Pashkevich

▶ **To cite this version:**

Yier Wu, Alexandr Klimchik, Stéphane Caro, Benoit Furet, Anatol Pashkevich. Geometric calibration of industrial robots using enhanced partial pose measurements and design of experiments. Robotics and Computer-Integrated Manufacturing, 2015, 35, pp.151-168. 10.1016/j.rcim.2015.03.007 . hal-01201694

HAL Id: hal-01201694

https://imt-atlantique.hal.science/hal-01201694v1

Submitted on 3 May 2018

HAL is a multi-disciplinary open access archive for the deposit and dissemination of scientific research documents, whether they are published or not. The documents may come from teaching and research institutions in France or abroad, or from public or private research centers.

L'archive ouverte pluridisciplinaire **HAL**, est destinée au dépôt et à la diffusion de documents scientifiques de niveau recherche, publiés ou non, émanant des établissements d'enseignement et de recherche français ou étrangers, des laboratoires publics ou privés.

Geometric calibration of industrial robots using enhanced partial pose measurements and design of experiments

Yier Wu [a,b], Alexandr Klimchik [a,b,*], Stéphane Caro [b], Benoît Furet [c], Anatol Pashkevich [a,b]

[a] Ecole des Mines de Nantes, 4 rue Alfred-Kastler, Nantes 44307, France
[b] CNRS, Institut de Recherches en Communications et et Cybernétique de Nantes, UMR CNRS 6597, 1 rue de la Noë, 44321 Nantes, France
[c] Université de Nantes, France

The paper deals with geometric calibration of industrial robots and focuses on reduction of the mea-surement noise impact by means of proper selection of the manipulator configurations in calibration experiments. Particular attention is paid to the enhancement of measurement and optimization techniques employed in geometric parameter identification. The developed method implements a complete and irreducible geometric model for serial manipulator, which takes into account different sources of errors (link lengths, joint offsets, etc). In contrast to other works, a new industry-oriented performance measure is proposed for optimal measurement configuration selection that improves the existing techniques via using the direct measurement data only. This new approach is aimed at finding the ca-libration configurations that ensure the best robot positioning accuracy after geometric error compen-sation. Experimental study of heavy industrial robot KUKA KR-270 illustrates the benefits of the devel-oped pose strategy technique and the corresponding accuracy improvement.

1. Introduction

In robotic literature, the problem of geometric calibration is already well studied and has been in the focus of the research community for many years [1–8]. As reported by a number of authors, the manipulator geometric errors are responsible for about 90% of the total positioning error [9]. Besides of the errors in link lengths and joint offsets, the end-effector positioning errors can be also caused by the non-perfect assembling of different links and arise in shifting and/or rotation of the frames associated with different elements, which are normally assumed to be matched and aligned [10]. It is clear that the geometric errors do not vary with the manipulator configuration, while their influence on the positioning accuracy depends on the latter. At present, there exist various calibration techniques that are able to calibrate the manipulator geometric model using different modeling, measurement and identification methods [11–16]. The identified errors can be efficiently compensated either by adjusting the controller input (the target point) or by direct modification of the model parameters used in the robot controller.

The classical calibration procedure usually includes four steps: modeling, measurement, identification and implementation. The *Modeling* step focuses on the development of proper geometric model of robotic manipulator. In the pioneer works [14], researches have used the classical DH convention for robot calibration. However, this model turned out to be discontinuous in some cases and may lead to unacceptable identification results [17]. So, several alternative approaches have been proposed to overcome these difficulties by means of introducing extra parameters [18,19]. Since the inclusion of additional parameters causes redundancy, these methods raise the problem of parameter non-identifiability, which leads to the necessity of investigating the model completeness, irreducibility and continuity. For example, in [20], the authors proposed a complete and parametrically continuous (CPC) model and further its modified version (MCPC) for robot calibration. Besides, there have been also proposed some analytical/numerical techniques for elimination of the non-identifiable parameters. For example, in [18], the authors used QR decomposition of the identification Jacobian for model reduction and in [21], the authors used straightforward evaluation of the Jacobian matrix rank.

The *Measurement* step involves data collecting of robot link and end-effector position/orientation. Generally, six parameters are required to specify the manipulator end-effector location (three translations and three rotations) [12,22], but sometimes the end-effector position is measured only [23]. Various calibration methods based on different measurement techniques were

* Corresponding author at: Ecole des Mines de Nantes, 4 rue Alfred-Kastler, Nantes 44307, France. Fax. +33 251 85 83 49.
E-mail address: alexandr.klimchik@mines-nantes.fr (A. Klimchik).

proposed, they are usually categorized as closed-loop and open-loop ones. The closed-loop calibration uses physical constraints on the manipulator end-link (point, line or plane constraints, for instance). It is claimed to be autonomous and does not require any external device [13,21,24]. However in this case, the manipulators must have some redundancy to perform self-motion, and the robot configuration should be carefully selected to satisfy particular constraints. Therefore, the open-loop methods have found wide applications; they are based on the full or partial pose measurements of the end-effector location using external devices. In practice, the partial pose information is often used and provides from one to five dimensional measurements [11,25,26] instead of the full pose information (6-dimensional location). In general, the lower dimensional measurement is more attractive due to simplicity of calibration experiment setup. For this so-called *partial pose measurement* technique, various external devices can be applied, such as laser tracking system [23], the ball-bar system [27] and wire potentiometer [22], etc.

The *identification* step in robot calibration can be treated as the best fitting of the experimental data (given input variables and measured output variables) by corresponding models. This problem has been addressed by a number of researchers who have used various modeling methods and identification algorithms, such as linear least square technique, Levenberg–Marquardt algorithm, Kalman filtering technique and maximum likelihood estimator etc. [16,28]. Among them, the least square technique is the most often applied one, which aims at minimizing the sum of squared residuals [29]. An important problem here is non-homogeneity of the residual errors (distances and angles, for instance). To solve this problem, usually a straightforward solution is applied: assigning weights or normalization, but this weight assigning procedure is very non-formal and not rigorous (while being essential for the final results). To solve the corresponding optimization problem, there exist various numerical algorithms such as gradient search [27,30], heuristic search and the others [31]. However, these numerical techniques are often difficult to apply due to large number of parameters to be tuned, that often lead to low convergence. Nevertheless, for the case of geometric calibration, the errors in the parameters are relatively small, so the linearization technique can be successfully applied. In this case, the solution of a linear least square problem can be found straightforwardly (i.e., via the pseudo-inverse of Moore–Penrose) [32,33]. It should be mentioned that in some particular cases, for instance, when the geometric errors are relatively large, the solution can only be found iteratively [15].

The most essential works on the above mentioned calibration methods in robotics literature are summarized in Table 1. Among these publications, limited number of works directly addresses the problem of parameter identification accuracy and reduction of the impact of measurement errors. Although the calibration accuracy may be improved by straightforwardly increasing the number of experiments [27], the measurement configurations may also affect the robot calibration [34]. It has been shown that the latter may significantly improve the identification accuracy [35]. Intuitively, using diverse manipulator configurations for different experiments seems perfectly corresponds to the basic idea of the classical experiment design theory, which intends to spread the measurements as much distinct as possible [15]. However, the classical results are mostly obtained for very specific models (such as the linear regression) and cannot be applied directly due to non-linearity of the relevant expressions of robot geometric model.

At present, there are few works where the problem of optimal pose selection for robot calibration has been discussed [39,40]. In these works, in order to compare the plans of experiments, several quantitative performance measures have been proposed and used as the objectives of the optimization problem associated with the optimal sets of measurement poses. In defining the objectives, the authors in [35,40–42] proposed some observability indices, which are based on the singular values of the identification Jacobian (condition number, for instance). These indices have been examined and compared in [38,39,43,44], where the authors paid more attention to developing efficient numerical algorithms, such as genetic algorithm, Tabu search, DETMAX and also hybrid methods in order to obtain the optimal measurement configurations. However, these approaches deal with rather abstract notions that are not directly related to the robot accuracy and may lead to some unexpected results, for example, when the condition number is good, but the parameter estimation errors are rather high. Besides, it usually requires very intensive and time consuming

Table 1
Summary of related works for geometric calibration

Application (Manipulator)	Number of model parameters	Number of measurement configurations	Measurement device	Identification algorithm	Achieved accuracy, [mm]
6-dof parallel robot [25]	35	80(1)	Two inclinometers(a)	Levenberg–Marquardt method	0.40
Stewart platform [36]	42	15(1)	Single theodolite(a)	Non-linear LS	0.50
PUMA 560 [23]	27	25(1)	Laser tracking system(a)	–	0.10
PUMA 560 [27]	36	800(1)	Ball-bar system(a)	Gradient search method	0.08
PUMA 560 [22]	24	48(1)	Wire potentiometer(a)	Non-linear LS	0.50
PUMA 560 [13]	23	100(3)	–(b)	Non-linear LS	0.25
Schilling Titan II [37]	42	800(2)	–(b)	Linear LS	5.70
Stäubli TX90 [15]	23	100(2)	Touching probe(b)	Weighted pseudo inverse	0.22
SCARA robot [38]	30	10(4)	–(b)	Genetic algorithm	3.60
Gough platform [39]	42	18(5)	Vision system(c)	Heuristic search	1.30

Selection of measurement configurations:

[1] Random configurations.
[2] Well distributed configurations.
[3] Noise amplification index.
[4] Minimum condition number.
[5] Several observability indices.

Measurement technique:

[a] Open-loop measurement.
[b] Closed-loop measurement.
[c] Simulation.

computations caused by a poor convergence and high dimension of the search space (number of calibration experiments multiplied by the manipulator joint number). Therefore, for the industrial applications, existing approaches should be essentially revised.

The *primary goal* of this work is to achieve the desired robot positioning accuracy using minimum number of experiments. Here it is proposed to introduce an additional step to the classical calibration procedure, the *design of experiments*, which is performed before measurements and is aimed at obtaining the set of measurements poses that ensures good calibration results (robot accuracy after error compensation). It allows us to improve the efficiency of error compensation and to estimate the robot accuracy, which is important for industrial applications.

To address the above mentioned problems, the remainder of the paper is organized as follows. Section 2 presents the problem of geometric calibration in general. Section 3 describes a suitable manipulator geometric model for calibration purposes (complete, irreducible model). Section 4 contains one of the main contributions: an enhanced partial pose measurement method. Section 5 describes a dedicated identification algorithm for manipulator geometric parameters. Section 6 proposes a new approach for optimal measurement pose selection and evaluates the calibration efficiency improvement. Section 7 presents the experimental results obtained for the geometric calibration of a KUKA KR-270 robot. Finally, Section 8 summarizes the main results and contributions of this paper.

2. Problem of geometric calibration

In robotics, calibration is a process that allows us to estimate the manipulator geometric parameters, which are employed in robot controller. In practice, the nominal values of these parameters are different from the real ones, so they should be identified for each particular manipulator using data from calibration experiments. As it was mentioned before, the conventional calibration procedure includes four sequential steps. In the scope of this paper, an additional step is introduced that deals with the design of calibration experiments, in order to improve the calibration accuracy. A relevant enhanced robot calibration procedure is presented in Fig. 1. The particularities of each step of this procedure are described below.

Step 1: This step deals with manipulator *modeling* and is aimed at developing a geometric model that is suitable for calibration (complete and irreducible), i.e. which is good enough from physical point of view and does not create any numerical problems during identification. This model should allow us to compute the end-effector location for any given values of the actuated joint coordinates q (provided that the manipulator parameters $\boldsymbol{\pi}$ are known). However, for calibration purposes, it is usually required a linearized version of this model allowing to evaluate the influence of the small variations of q and $\boldsymbol{\pi}$. So let us assume that the manipulator links are rigid and corresponding geometric model can be written as the vector function $t=g(q, \boldsymbol{\pi})$, where $t=(p, \boldsymbol{\varphi})^T$ defines the manipulator end-effector location (position and orientation), vector q contains all actuated joint coordinates, and vector $\boldsymbol{\pi} = \boldsymbol{\pi}_0 + \Delta\boldsymbol{\pi}$ collects all geometric parameters and their

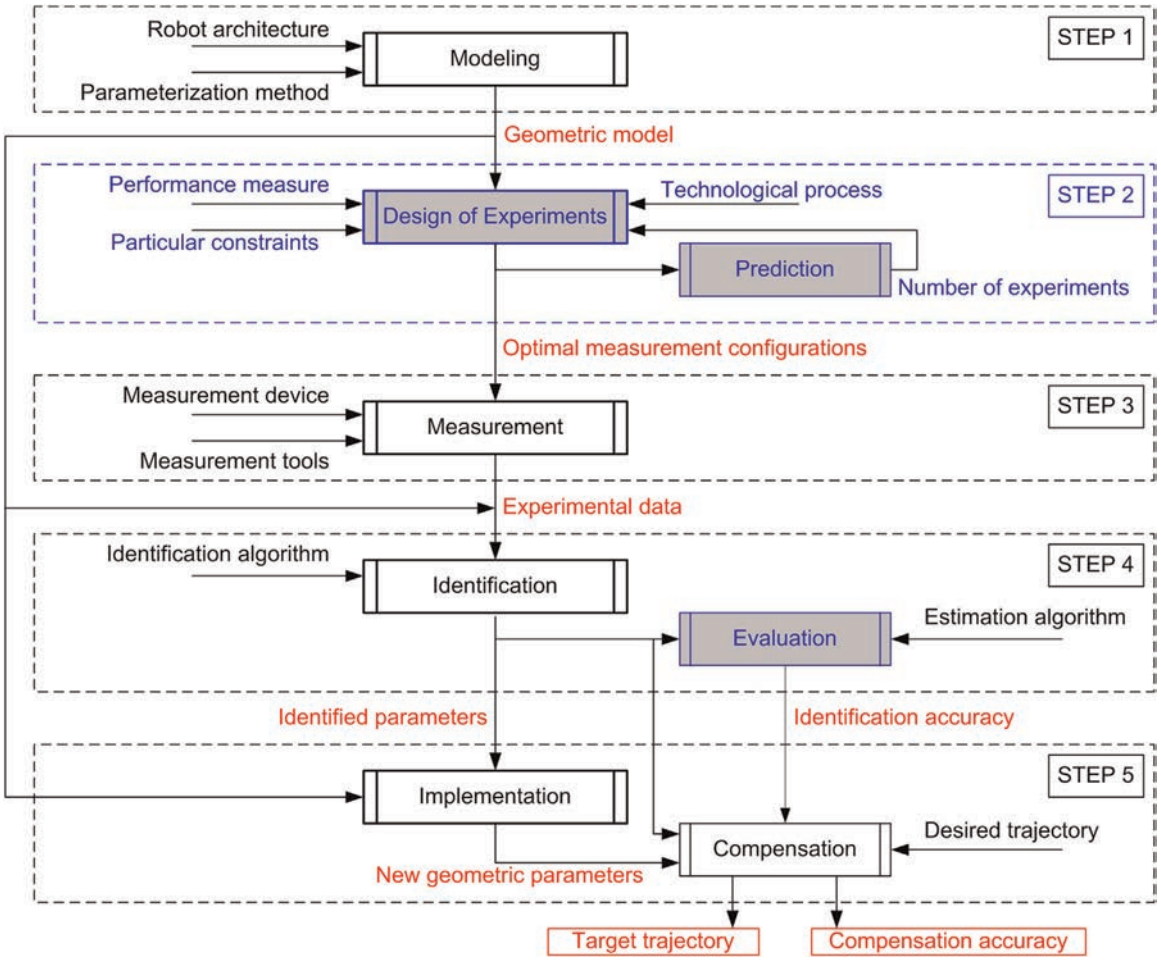

Fig. 1. Enhanced robot calibration procedure.

deviations. Under this assumption, the actual location of the manipulator end-effector, which incorporates the geometric errors is expressed as $t=g(q, \boldsymbol{\pi}_0 + \Delta\boldsymbol{\pi})$. In practice, the geometric errors $\Delta\boldsymbol{\pi}$ are usually relatively small, therefore the following linerized model can be used

$$t=t_0 + J_\pi \Delta\boldsymbol{\pi} \tag{1}$$

where $t_0 = g(q, \boldsymbol{\pi}_0)$ is the end-effector location computed using the nominal geometric parameters, $J_\pi$is the identification Jacobian matrix, which can be computed using the derivative $\partial g(q, \boldsymbol{\pi}_0)/\partial\boldsymbol{\pi}$. More details concerning the computation of identification Jacobian can be found in [45].

Step 2: This is an additional step (*design of experiments*) that is introduced here in the calibration procedure. It is aimed at choosing optimal measurement configurations for calibration experiments. It should rely on an appropriate performance measure, which takes into account the particularities of the technological process (robotic-based machining, for instance). It should be also able to obtain solution within the work-cell constraints, and to adjust the number of experiments with respect to the measurement system precision. In practice, the influence of the geometric errors on the end-effector position varies from one configuration to another and essentially differs throughout the workspace. So, the desired accuracy is usually required to be achieved for rather limited workspace area (for example, where the workpieces are located in the robotic cell). For this reason, in this paper, it is proposed to limit the benchmark manipulator configurations by a single one (the machining configuration, for instance), which will be further referred to as the *manipulator test-pose*. To develop a new approach of calibration experiments design that utilizes the above proposed ideas, let us introduce several basic definitions:

Definition 1. The *plan of experiments* is a set of manipulator configurations $\{q_i, i = \overline{1, m}\}$ that are used for the measurements of the end-effector positions $\{p_i^j, i = \overline{1, m}, j = \overline{1, n}\}$ and for further identification of the desired parameters $\boldsymbol{\pi}$.

Definition 2. The *manipulator test-pose* is a particular robot configuration q_0 (that is usually specified in relevant technological process), for which it is required to achieve the best compensation of the end-effector positioning errors.

Definition 3. The *quality of the plan of experiments* is defined by the efficiency of manipulator positioning error compensation at the test-pose, which is the root-mean-square distance ρ_0 between the desired manipulator end-effector position and the position obtained after error compensation.

Step 3: This step (*measurements*) deals with carrying out calibration experiments using the obtained configurations. Depending on the measurement methods (measurement tools and devices, reference point locations, see Fig. 2, where a typical manipulator mounting flange is shown), it may provide different experimental data (the end-effector position/location, etc.). For the conventional full-pose measurement technique that is frequently used in robot calibration, the corresponding optimization problem allowing us to compute the desired parameters is expressed as

$$\sum_{i=1}^{m} \|\Delta t_i - J_{\pi i}\Delta\boldsymbol{\pi}\|^2 \to \min_{\Delta\boldsymbol{\pi}} \tag{2}$$

However, the residual components of this system of identification equations are non-homogeneous (millimeters and radians, for instance). In some cases, these components are normalized before computing the squared sum, but it is a non-trivial step that affects the identification accuracy. To overcome this difficulty, it is proposed to enhance the partial pose measurement method that uses directly and only the positioning coordinates, but for several reference points for each manipulator configuration. More details of this method and its advantages will be presented in Section 4.

Step 4: This step deals with the *identification* and is aimed at estimating the geometric parameters by using the corresponding model and proper identification algorithm. Usually, the identification algorithms are based on the minimization of the least-square objectives that are derived assuming that the measurement tool has a single reference point (see Eq.(2)), while the proposed measurement technique operates with several of them. For this reason, it is required to revise the existing identification techniques, taking into account both modification of the objective function and increasing of the number of parameters (since each reference point introduces additional parameters).

In addition, this step includes the evaluation of the parameter identification accuracy. In practice, different sources of error may affect the identification precision. They include the measurement errors of the external device providing the end-effector position coordinates (laser tracker in our case), the errors in the actuator encoders (internal measurement devices) giving the manipulator joint coordinates that depend on encoder resolution, etc. Besides, the assumption concerning the manipulator model (the link rigidity, for instance) may also affect the identification accuracy. It is clear that, all these sources of error can be hardly taken into account in calibration. For this reason, only the most significant of the above mentioned sources of error should be considered in the accuracy analysis. As follows from our experience, the inaccuracy of external measurement system has the most significant impact on the robot positioning accuracy, comparing to other sources of error that can be assumed negligible in the frame of geometric calibration.

Step 5: At the last step (*implementation*), the geometric errors are compensated by modification of the geometric parameter values embedded in the robot controller. In the case when some errors cannot be entered in the controller directly, an off-line error compensation technique is required. This technique should compensate the manipulator errors via modification of the target trajectory that becomes slightly different from the desired one [46].

It is clear that the proposed scheme of robot calibration procedure allows us to improve the calibration accuracy for given number of experiments (or to minimize the number of experiments for given accuracy). The steps 1, 4 and 5 in the calibration procedure have been already well studied [9,47], while the steps 2 and 3 still require some revision in terms of the applicability to particular manufacturing process where the robot is used. Hence, the goal of this work is the enhancement of calibration technique for manipulator geometric parameters using enhanced partial pose measurement and design of experiments. Particular

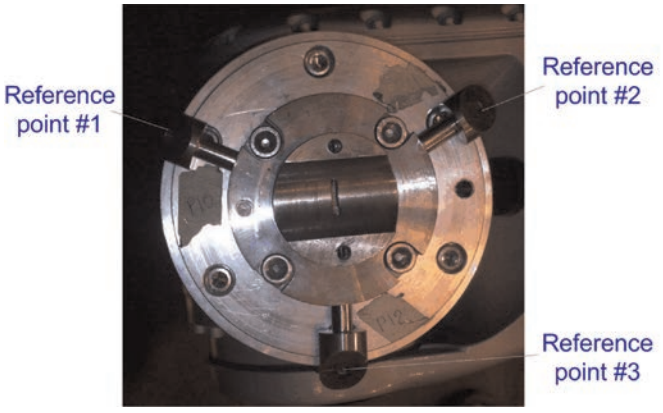

Fig. 2. Measurement tool with several reference points.

problems that should be considered are the following:

(1) Development of an industry-oriented performance measure which has clear physical meaning that is related to the robot accuracy after geometric error compensation.
(2) Enhancement of partial pose measurement method that allows us to avoid the problem of non-homogeneity in the identification equations.
(3) Experimental validation of the developed approach for geometric calibration of an industrial KUKA KR-270 robot.

These problems will be considered in more details in the following sections.

3. Manipulator geometric modeling

To be suitable for robot calibration, the manipulator geometric model must satisfy certain requirements. In particular, it should be complete, i.e. is able to describe all possible errors in link/joint geometry, but not redundant (i.e. does not contain parameters that influence the end-effector position/orientation in the same way for any manipulator configuration). In previous works [48] [49], it was shown that the conventional D-H model may produce problems for parameter identification because its incompleteness. To avoid this difficulty, some modifications have been proposed that however introduce some redundancy, which may cause non-identifiability of certain parameters. This redundancy can be eliminated by applying either numerical or analytical techniques [20,21,50] that allow us to obtain an appropriate model, which is usually referred to as "complete, irreducible and continuous" one. Let us apply one of these techniques [51] to generate the desired model for heavy industrial manipulator KUKA KR-270 that will be used in experimental study.

In the frame of the above defined notations and assuming that the manipulator links are rigid enough and the non-geometric factors are negligible in this level of calibration, the general expression of the geometric model for a n-dof serial manipulator can be described as a sequence of homogeneous transformations

$$\mathrm{T}(\mathrm{q}) = \mathrm{T}_{base}(\boldsymbol{\pi}_b)\cdot\left[\mathrm{T}_{\mathrm{Joint}}(q_1,\pi_{q1})\cdot\mathrm{T}_{Link}(\boldsymbol{\pi}_{L1})\right]\cdot\ldots \cdot\left[\mathrm{T}_{\mathrm{Joint}}(q_n,\pi_{qn})\cdot\mathrm{T}_{Link}(\boldsymbol{\pi}_{Ln})\right]\cdot\mathrm{T}_{tool}(\boldsymbol{\pi}_t) \quad (3)$$

where T with different indices denote the relevant transformation matrices of size 4×4, q is the vector of the actuated joint coordinates, while the vectors $\boldsymbol{\pi}_b$, $\boldsymbol{\pi}_t$, $\boldsymbol{\pi}_{Lj}$ and the scalars π_{qj} are the manipulator geometric parameters corresponding to the base, tool, links and joints, respectively. In the literature, there are a number of techniques that allows us to obtain the manipulator model of such type, which is definitely complete but includes redundant parameters to be eliminated (methods of Hayati, Whitney–Losinski, etc.). In this work, we will use the model generation technique that is based on dedicated analytical elimination rules and includes the following steps:

Step 1. Construction of the complete and reducible model in the form of homogeneous matrices product.

- The base transformation $\mathrm{T}_{base} = \left[\mathrm{T}_x\mathrm{T}_y\mathrm{T}_z\mathrm{R}_x\mathrm{R}_y\mathrm{R}_z\right]_b$
- The joint and link transformations $\mathrm{T}_{\mathrm{Joint},j}\cdot\mathrm{T}_{Link,j}$
  (1) For revolute joint $\mathrm{T}_{\mathrm{Joint},j}\cdot\mathrm{T}_{Link,j} = \mathrm{R}_{e,j}(q_j, \pi_{qj})\cdot[\mathrm{T}_u\mathrm{T}_v\mathrm{R}_u\mathrm{R}_v]_{Lj}$
  (2) For prismatic joint $\mathrm{T}_{\mathrm{Joint},j}\cdot\mathrm{T}_{Link,j} = \mathrm{T}_{e,j}(q_j, \pi_{qj})\cdot[\mathrm{R}_u\mathrm{R}_v]_{Lj}$

  where $\mathrm{e}_j$is the joint axis, u_j and v_j are the axes orthogonal to e_j.

- The tool transformation $\mathrm{T}_{tool} = \left[\mathrm{T}_x\mathrm{T}_y\mathrm{T}_z\mathrm{R}_x\mathrm{R}_y\mathrm{R}_z\right]_t$

Step 2. Elimination of non-identifiable and semi-identifiable parameters in accordance with specific rules for different nature and structure of consecutive joints.

- For the case of consecutive revolute joint $\mathrm{R}_{e,j}(q_j, \pi_{qj})$
  (1) if $\mathrm{e}_j\perp\mathrm{e}_{j-1}$, eliminate the term $\mathrm{R}_{u,Lj-1}$ or $\mathrm{R}_{v,Lj-1}$ that corresponds to $\mathrm{R}_{e,j}$;
  (2) if $\mathrm{e}_j\|\mathrm{e}_{j-1}$, eliminate the term $\mathrm{T}_{u,Lj-k}$ or $\mathrm{T}_{v,Lj-k}$that defines the translation orthogonal to the joint axes, for which k is minimum ($k \geq 1$).
- For the case of consecutive prismatic joint $\mathrm{T}_{e,j}(q_j, \pi_{qj})$
  (1) if $\mathrm{e}_j\perp\mathrm{e}_{j-1}$, eliminate the term $\mathrm{T}_{u,Lj-1}$ or $\mathrm{T}_{u,Lj-1}$ that corresponds to $\mathrm{T}_{e,j}$;
  (2) if $\mathrm{e}_j\|\mathrm{e}_{j-1}$, eliminate the term $\mathrm{T}_{u,Lj-k}$ or $\mathrm{T}_{v,Lj-k}$that defines the translation in the direction of axis e_j, for which k is minimum ($k \geq 1$).

Let us apply the above presented technique to the industrial robot KUKA KR-270 (See Fig. 3), which is used in experimental validations of this paper. For this manipulator that includes six revolute joints, the complete (but redundant) model contains 42 parameters and can be presented as

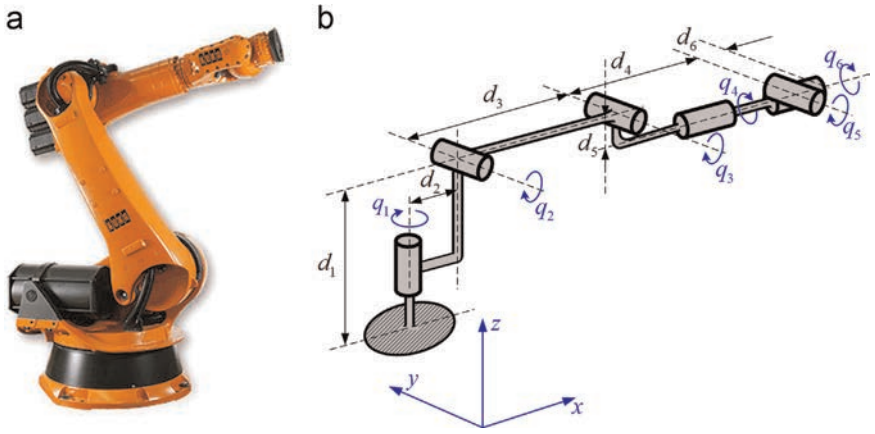

Fig. 3. The industrial serial robot KUKA KR-270 and its geometric parameters. (a) Industrial robot KUKA KR270 and (b) the manipulator architecture.

$$\mathrm{T}=\left[\mathrm{T}_x\mathrm{T}_y\mathrm{T}_z\mathrm{R}_x\mathrm{R}_y\mathrm{R}_z\right]_b\cdot\mathrm{R}_z(q_1+\Delta q_1)\cdot\left[\mathrm{T}_x\mathrm{T}_y\mathrm{R}_x\mathrm{R}_y\right]_{L1}$$
$$\cdot\mathrm{R}_y(q_2+\Delta q_2)\cdot[\mathrm{T}_x\mathrm{T}_z\mathrm{R}_x\mathrm{R}_z]_{L2}\cdot$$
$$\cdot\,\mathrm{R}_y(q_3+\Delta q_3)\cdot[\mathrm{T}_x\mathrm{T}_z\mathrm{R}_x\mathrm{R}_z]_{L3}\cdot\mathrm{R}_x(q_4+\Delta q_4)$$
$$\cdot\left[\mathrm{T}_y\mathrm{T}_z\mathrm{R}_y\mathrm{R}_z\right]_{L4}\cdot\mathrm{R}_y(q_5+\Delta q_5)\cdot[\mathrm{T}_x\mathrm{T}_z\mathrm{R}_x\mathrm{R}_z]_{L5}$$
$$\cdot\,\mathrm{R}_x(q_6+\Delta q_6)\cdot\left[\mathrm{T}_y\mathrm{T}_z\mathrm{R}_y\mathrm{R}_z\right]_{L6}\cdot\left[\mathrm{T}_x\mathrm{T}_y\mathrm{T}_z\mathrm{R}_x\mathrm{R}_y\mathrm{R}_z\right]_t \tag{4}$$

It should be mentioned that the nominal values of some parameters can be found in the manufacturer datasheets, but the remaining ones are assumed to be equal to zero. Applying the elimination rules for the case of consecutive revolute joints, the parameters $\left\{\mathrm{R}_{y,L1}, \mathrm{T}_{z,L2}, \mathrm{R}_{x,L3}, \mathrm{R}_{y,L4}, \mathrm{T}_{x,L5}, \mathrm{R}_{x,L5}\right\}$ are sequentially eliminated from the redundant model (4). Here, it is worth making the following remarks:

Remark 1. In the redundant model (4), it has been already taken into account that the nominal geometric parameter d_1 (shift of the robot base along z-axis) cannot be identified separately from the base transformation.

Remark 2. For the first and the last joints, which are connected to the robot base and tool respectively, the offsets Δq_1 and Δq_6 are treated as semi-identifiable parameters. So, they are eliminated from the manipulator geometric model and are incorporated in the base and tool parameters. However, the actuated joint variables q_1 and q_6 must retain in the model.

Remark 3. The geometric parameters of the last link $\left\{\mathrm{T}_y, \mathrm{T}_z, \mathrm{R}_y, \mathrm{R}_z\right\}_{L6}$ cannot be identified separately from the tool transformation. So, it is reasonable to include these parameters in the tool transformation.

Remark 4. In the case when only position measurements are available, the tool orientations are not known. So, the parameters of the rotational transformations $\left\{\mathrm{R}_x, \mathrm{R}_y, \mathrm{R}_z\right\}_t$ corresponding to the tool are treated as non-identifiable.

Remark 5. Six parameters describing the base transformation $\left\{\mathrm{T}_x, \mathrm{T}_y, \mathrm{T}_z, \mathrm{R}_x, \mathrm{R}_y, \mathrm{R}_z\right\}_b$ and three parameters $\left\{\mathrm{T}_x, \mathrm{T}_y, \mathrm{T}_z\right\}_t$ that define tool transformation can be treated as known (there are dedicated techniques to identify them separately).

This finally allows us to obtain the complete and irreducible geometric model for the considered manipulator that includes 18 principle parameters to be identified.[1]

$$\mathrm{T}_{robot}=\mathrm{R}_z(q_1)\cdot\left[\mathrm{T}_x\mathrm{T}_y\mathrm{R}_x\right]_{L1}$$
$$\cdot\mathrm{R}_y(q_2+\Delta q_2)\cdot[\mathrm{T}_x\mathrm{R}_x\mathrm{R}_z]_{L2}\cdot\mathrm{R}_y(q_3+\Delta q_3)\cdot[\mathrm{T}_x\mathrm{T}_z\mathrm{R}_z]_{L3}$$
$$\cdot\,\mathrm{R}_x(q_4+\Delta q_4)\cdot\left[\mathrm{T}_y\mathrm{T}_z\mathrm{R}_z\right]_{L4}\cdot\mathrm{R}_y(q_5+\Delta q_5)\cdot[\mathrm{T}_z\mathrm{R}_z]_{L5}\cdot\mathrm{R}_x(q_6) \tag{5}$$

This model will be further used for geometric calibration of the industrial robot KUKA KR-270 and for the optimal selection of the measurement poses. Let us collect these parameters in the following vector

$$\boldsymbol{\pi}=\left\{p_{x1}\ p_{y1}\ \varphi_{x1}\ \Delta q_2\ p_{x2}\ \varphi_{x2}\ \varphi_{z2}\ \Delta q_3\ p_{x3}\ p_{z3}\ \varphi_{z3}\ \Delta q_4\ p_{y4}\ p_{z4}\ \varphi_{z4}\right.$$
$$\left.\Delta q_5\ p_{z5}\ \varphi_{z5}\right\} \tag{6}$$

[1] It should be stressed that 6 parameters related to the base transformation and 6 parameters describing the tool transformation are not included in this expression (see Remarks 1 and 5), so it is in good agreement with common expression of Zhuang [52] that for robot with 6 rotational joints yields 30 independent parameters.

where Δq_j is the joint offset, p_{xj}, p_{yj}, p_{zj} and φ_{xj}, φ_{yj}, φ_{zj} are the relevant translational and rotational parameters, and j indicates the joint/link number. For these parameters, the corresponding nominal values are

$$\boldsymbol{\pi}_0=\left\{d_2\ \ 0\ \ 0\ \ 0\ \ d_3\ \ 0\ \ 0\ \ 0\ \ d_4\ \ d_5\ \ 0\ \ 0\ \ 0\ \ 0\ \ 0\ \ 0\ \ 0\right\} \tag{7}$$

where the geometric meaning of d_2, ... , d_5 is illustrated in Fig. 3. In the following sections, this model will be used for computing the end-effector location of the KUKA KR-270 robot required for some numerical routines employed in parameter identification algorithms.

4. Enhanced partial pose measurement method

In industrial applications, it is often used the partial pose measurement method that requires obtaining the end-effector position coordinates only (without orientation). On the other hand, this simplification does not allow the user to identify certain manipulator parameters that can be estimated via the end-effector orientation. For this reason, this section presents an intermediate technique, where the orientation is not computed directly but is incorporated in the identification equations via the Cartesian coordinates of several reference points.

For the *conventional full pose measurement technique*, the desired parameters are identified from the full-scale linearized geometric model (1), which can be rewritten as

$$\Delta\mathrm{t}_i=\mathrm{J}_{\pi i}\Delta\boldsymbol{\pi},\ \ i=1, 2, \dots m \tag{8}$$

where $\Delta\mathrm{t}_i=(\Delta p_{xi}, \Delta p_{yi}, \Delta p_{zi}, \Delta\varphi_{xi}, \Delta\varphi_{yi}, \Delta\varphi_{zi})^T$ is the pose deviation caused by small variation in the model parameters $\Delta\boldsymbol{\pi}$. It is clear that the corresponding system of linear equations can be solved with respect to $\Delta\boldsymbol{\pi}$ if the number of experiments m is sufficiently high and the manipulator configurations $\{\mathrm{q}_i,\ i=1, m\}$ are different to ensure non-singularity of relevant observation matrix used in the identification procedure. For this technique, each configuration q_i produces six scalar equations to be used for the identification. Corresponding optimization problem (2) whose solution leads to the desired parameters $\Delta\boldsymbol{\pi}$ is often solved without paying attention to the non-homogeneity of the residual components. In some cases, the weighted least-square technique is used to resolve this problem, but the weighting coefficients are usually defined intuitively, which may affect essentially the identification accuracy.

The main difficulty of this conventional technique (full-pose) is that the orientation components $(\varphi_{xi}.\ \varphi_{yi}.\ \varphi_{zi})^T$ cannot be measured directly. So, these angles are computed using excessive number of measurements for the same configuration q_i, which produce Cartesian coordinates $\{(p_{xi}^j, p_{yi}^j, p_{zi}^j)^T |\ j=\overline{1, n}\ ;\ n\geq 3\}$ for several reference points of the measurement tool attached to the manipulator mounting flange (Fig. 2). Hence, instead of using $3mn$ scalar equations, that can be theoretically obtained from the measurement data, this conventional approach uses only $6m$ scalar equations for the identification. This may obviously lead to some loss of the parameter estimation accuracy.

To overcome this difficulty, *the proposed technique* is based on reformulation of the optimization problem (2) using only the data directly available from the measurement system, i.e. the Cartesian coordinates of all reference points p_i^j (see Fig. 2). This idea allows us to obtain homogeneous identification equations where each residual has the same unit (mm, for instance), and the optimization problem is rewritten as follows

$$\sum_{i=1}^{m}\sum_{j=1}^{n}\left\|\Delta\mathrm{p}_i^j-\mathrm{J}_{\pi i}^{j(p)}\Delta\boldsymbol{\pi}\right\|^2\rightarrow\min_{\Delta\boldsymbol{\pi}} \tag{9}$$

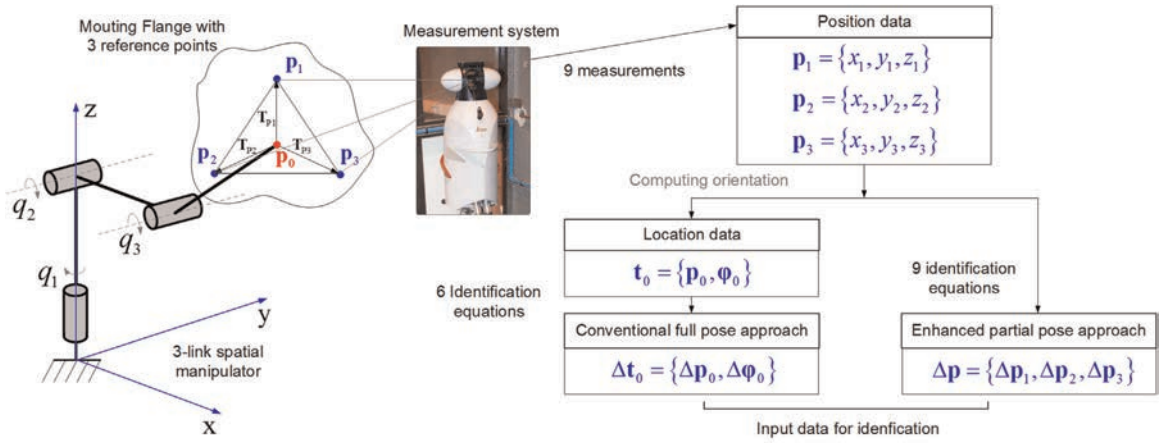

Fig. 4. Difference between conventional full-pose approach and enhanced partial pose approache.

Here, the matrix $J_{\pi i}^{j(p)}$ with the superscripts "(p)" denotes the position rows of the corresponding identification Jacobian $J_{\pi i}^{j}$, the index "i" defines the manipulator configuration number, and the index "j" denotes the reference point number. An obvious advantage of this formulation is its simplicity and clarity of the residual vector norm definition (conventional Euclidian norm can be applied here reasonably, the normalization is not required). So, the problem of the weighting coefficient selection does not exist in this case. In fact, under the assumption that measurement errors are modeled as a set of independent and identically distributed (i.i.d.) random values (similar for all directions x, y, z and for all measurement configurations), the optimal linear estimator should operate with equal weights for all equations. Besides, the most important issue is related to the potential benefits in the identification accuracy, since the total number of scalar equations incorporated in the least-square objective increases from $6m$ to $3mn$.

To compare the efficiency of the presented approach with the conventional one, a simulation study has been carried out, which dealt with geometric calibration of a 3-link spatial manipulator (Fig. 4). Detail description of this example can be found in [53], where it has been proved that the enhanced technique based on partial pose information ensures essential improvement of parameter identification accuracy. Using these identified geometric parameters, it is possible to evaluate the manipulator end-effector positioning accuracy throughout the workspace. Corresponding results are shown in Fig. 4, in which the achieved robot accuracy has been compared for two techniques. As follows from this figure, using the proposed approach, the maximum positioning error has not even reached the minimum one by using conventional technique. Moreover, the minimum positioning error has been reduced by a factor of 4. Fig. 5

Therefore, the partial pose technique is rather promising and will be further used for calibration experiments in this work. In contrast to the conventional methods, this technique allows us to avoid the problem of non-homogeneity of the relevant optimization objective and does not require any normalization (which arises in the case when full pose residuals are used).

5. Identification of manipulator geometric parameters

5.1. Identification algorithm for the enhanced partial pose method

Let us assume that the measurement tool has n reference points ($n \geq 3$) that are used to estimate relevant vectors of the Cartesian coordinates $\mathrm{p}_i^j = (p_{xi}^j, p_{yi}^j, p_{zi}^j)^T$ for m manipulator configurations q_i. In this notation, the subscript "i" and subscript "j" denote the experiment number and reference point number respectively. Correspondingly, the manipulator geometric model (3) can be rewritten as

$$\mathrm{T}_i^j = \mathrm{T}_{base} \cdot \mathrm{T}_{robot}(\mathrm{q}_i, \boldsymbol{\pi}) \cdot \mathrm{T}_{tool}^j; \;\; i = \overline{1, m}, \;\; j = \overline{1, n} \tag{10}$$

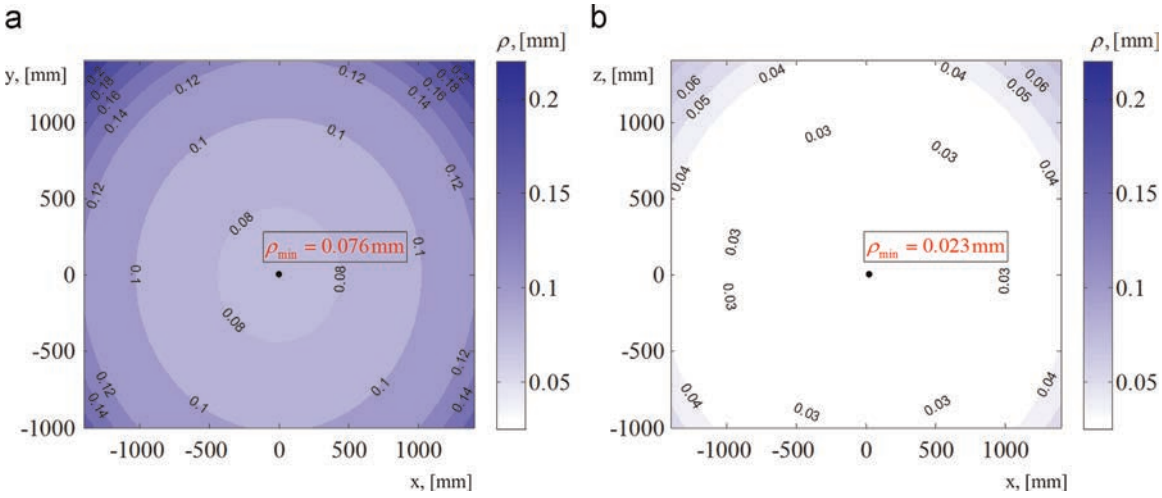

Fig. 5. Improvement of manipulator positioning accuracy after calibration due to the enhanced partial pose technique: (a) Conventional technique and (b) proposed technique.

where the vectors p_i^j are incorporated in the fourth column of the homogenous transformation matrix T_i^j, the matrix T_{base} defines the robot base location, the matrices T_{tool}^j, $j = \overline{1, n}$ describe the locations of the reference points that are observed by the measurement system (see Fig. 2). Here, the matrix function $T_{robot}(q_i, \boldsymbol{\pi})$ describes the manipulator geometry and depends on the current values of the actuated coordinates q_i and the parameters $\boldsymbol{\pi}$ to be estimated. Taking into account that any homogeneous transformation matrix T_a^b can be split into the rotational R_a^b and translational p_a^b components and presented as

$$T_a^b = \begin{bmatrix} R_a^b & p_a^b \\ \mathbf{0} & 1 \end{bmatrix}, \tag{11}$$

the vector of the reference point positions p_i^j, $j = \overline{1, n}$ (that are measured in the calibration experiments) can be expressed in the following form

$$p_i^j = p_{base} + R_{base} \cdot p_{robot}(q_i, \boldsymbol{\pi}) + R_{base} \cdot R_{robot}(q_i, \boldsymbol{\pi}) \cdot p_{tool}^j;$$
$$i = \overline{1, m}, j = \overline{1, n}. \tag{12}$$

This allows us to obtain $3mn$ scalar equations for the calibration purposes, where $n \geq 3$ and m is high enough to ensure identifiability of the desired parameters.

Applying the least-square method, the corresponding optimization problem can be presented as

$$\sum_{i=1}^{m} \sum_{j=1}^{n} \| p_i^j - p_{base} - R_{base} \cdot p_{robot}(q_i, \boldsymbol{\pi}) - R_{base} \cdot R_{robot}(q_i, \boldsymbol{\pi}) \cdot p_{tool}^j \|^2 \rightarrow \min_{\{p_{base}, R_{base}, p_{tool}^j, \boldsymbol{\pi}\}} \tag{13}$$

where the vectors/matrices p_{base}, R_{base}, $\left\{p_{tool}^j, j = \overline{1, n}\right\}$ and $\boldsymbol{\pi}$ are treated as unknowns.

The main difficulty with this optimization problem is that some of the unknowns are included in the objective function in highly non-linear way. So, to solve this problem, numerical optimization technique is required. However in practice, the deviations in the model parameters are relatively small, which allows us to linearize the manipulator geometric model (12). This leads to a linear least-square problem, whose solution can be obtained straightforwardly with the matrix pseudo-inverse. However, to simplify computations, here it is proposed to apply the linearization technique sequentially and separately with respect to two different subsets of the model parameters (corresponding to the base/tool transformations and the manipulator geometry). Consequently, the identification procedure is split into two steps. In the frame of this approach, the first step deals with the estimation of p_{base}, R_{base}, p_{tool}^j, which are related to the base and tool transformations (assuming that the manipulator parameters are known). The second step focuses on the estimation of $\boldsymbol{\pi}$ under the assumption that the base and tool components have been already identified. In order to ensure that the desired identification accuracy can be achieved, these two steps are repeated iteratively.

Step 1. For the first step, taking into account that the errors in the base orientation are relatively small, the matrix R_{base} is presented in the following form

$$R_{base} = [\sim \boldsymbol{\varphi}_{base}] + I \tag{14}$$

where I is a 3×3 identity matrix, vector $\boldsymbol{\varphi}_{base}$ includes the deviations in the base orientation angles, and the operator "[~]" transforms the vector $\boldsymbol{\varphi} = (\varphi_x, \varphi_y, \varphi_z)^T$ into the skew symmetric matrix as

$$[\sim \boldsymbol{\varphi}] = \begin{bmatrix} 0 & -\varphi_z & \varphi_y \\ \varphi_z & 0 & -\varphi_x \\ -\varphi_y & \varphi_x & 0 \end{bmatrix} \tag{15}$$

This leads to the following simplified expression of Eq. (12)

$$p_i^j = p_{base} + p_{robot}^i - p_{robot}^i \cdot [\sim \boldsymbol{\varphi}_{base}] + R_{robot}^i \cdot u_{tool}^j \tag{16}$$

that can also be rewritten in a matrix form as

$$p_i^j = p_{robot}^i + \begin{bmatrix} I & \left[\sim p_{robot}^i\right]^T & R_{robot}^i \end{bmatrix} \begin{bmatrix} p_{base} \\ \boldsymbol{\varphi}_{base} \\ u_{tool}^j \end{bmatrix} \tag{17}$$

and

$$u_{tool}^j = R_{base} p_{tool}^j \tag{18}$$

Here the vectors p_{base}, $\boldsymbol{\varphi}_{base}$ and u_{tool}^j, $j = \overline{1, n}$ are treated as unknowns.

Applying to the linear system (17) the linear least-square technique, the desired vectors defining the base and tool transformation parameters can be expressed as follows

$$\left[p_{base}; \boldsymbol{\varphi}_{base}; u_{tool}^1; \ldots u_{tool}^n\right] = \left(\sum_{i=1}^{m} A_i^{jT} A_i^j\right)^{-1} \left(\sum_{i=1}^{m} A_i^{jT} \Delta p_i\right) \tag{19}$$

where

$$A_i^j = \begin{bmatrix} I & \left[\sim p_{robot}^i\right]^T & R_{robot}^i & \mathbf{0} & \ldots & \mathbf{0} \\ I & \left[\sim p_{robot}^i\right]^T & \mathbf{0} & R_{robot}^i & \ldots & \mathbf{0} \\ \ldots & \ldots & \ldots & \ldots & \ldots & \ldots \\ I & \left[\sim p_{robot}^i\right]^T & \mathbf{0} & \mathbf{0} & \ldots & R_{robot}^i \end{bmatrix} \tag{20}$$

and the residuals are integrated in a single vector $\Delta p_i = (\Delta p_i^1, \ldots, \Delta p_i^n)^T$. Finally, the variables defining the location of the reference points are computed using Eq. (18) as $p_{tool}^j = R_{base}^T \cdot u_{tool}^j$. This allows us to find the homogeneous transformation matrices T_{base} and T_{tool}^j that are contained in Eq. (10).

Step 2. On this step, the manipulator geometric parameters $\boldsymbol{\pi}$ are estimated. For this purpose, the principal system (10) is linearized and rewritten in the form

$$\Delta p_i^j = J_{\pi i}^{j(p)} \cdot \Delta \boldsymbol{\pi} \tag{21}$$

where $\Delta p_i^j = p_i^j - p_{robot}^i$ is the residual vector corresponding to the j–th reference point for the i–thmanipulator configuration, $\Delta \boldsymbol{\pi}$ is the vector of geometric errors, the matrix $J_{\pi i}^j$ is the identification Jacobian computed for the configuration q_i with respect to the reference point j. Applying to this system the least-square technique, the desired vectors of geometric errors $\Delta \boldsymbol{\pi}$ can be obtained as

$$\Delta \boldsymbol{\pi} = \left(\sum_{i=1}^{m} \sum_{j=1}^{n} J_{\pi i}^{j(p)T} J_{\pi i}^{j(p)}\right)^{-1} \left(\sum_{i=1}^{m} \sum_{j=1}^{n} J_{\pi i}^{j(p)T} \Delta p_i^j\right) \tag{22}$$

It should be noted that, to achieve the desired accuracy for the original non-linear problem (13), the steps 1 and 2 should be repeated iteratively.

Another particularity may arise here is related to the property of measurement noise. In the above expressions, it was explicitly assumed that the measurement errors are similar for all directions. However, for some measurement systems, the errors in the longitudinal and transversal directions may essentially differ. In this case, the Eqs. (19) and (22) should be slightly modified by

including weighting coefficients

$$\left[\mathrm{p}_{base};\ \boldsymbol{\varphi}_{base};\ \mathrm{u}^1_{tool};\ \ldots\ \mathrm{u}^n_{tool}\right] = \left(\sum_{i=1}^{m} \mathrm{A}_i^{jT}\mathrm{W}_i^{j2}\mathrm{A}_i^{j}\right)^{-1}\left(\sum_{i=1}^{m} \mathrm{A}_i^{jT}\mathrm{W}_i^{j2}\Delta\mathrm{p}_i\right) \tag{23}$$

and

$$\Delta\boldsymbol{\pi} = \left(\sum_{i=1}^{m}\sum_{j=1}^{n} \mathrm{J}_{\pi i}^{j(p)T}\mathrm{W}_i^{j2}\mathrm{J}_{\pi i}^{j(p)}\right)^{-1}\left(\sum_{i=1}^{m}\sum_{j=1}^{n} \mathrm{J}_{\pi i}^{j(p)T}\mathrm{W}_i^{j2}\Delta\mathrm{p}_i^{j}\right) \tag{24}$$

where the weighting coefficients matrix W_i^j is computed using a technique proposed in our previous work [54].

Hence, the above presented identification algorithm is able to provide the estimation of the manipulator geometric parameters as well as the matrices of the base and tool transformations. However, the obtained identification results usually include some dispersion due to measurement errors. So, in order to achieve desired identification accuracy, the influence of these errors should be evaluated and reduced as much as possible, which will be in the focus of the following subsection.

5.2. Influence of the measurement errors on the identification accuracy

Under the assumption that measurement noise has the most significant impact on the robot positioning accuracy and the other sources of error are negligible, the basic equation of calibration (21) should integrate the measurement errors and is expressed as

$$\Delta\mathrm{p}_i^j = \mathrm{J}_{\pi i}^{j(p)}\cdot\Delta\boldsymbol{\pi} + \boldsymbol{\varepsilon}_i^j;\ i = \overline{1, m},\ j = \overline{1, n} \tag{25}$$

where the vectors $\boldsymbol{\varepsilon}_i^j = (\varepsilon_{xi}^j, \varepsilon_{yi}^j, \varepsilon_{zi}^j)^T$ denote the additive random errors, which are usually assumed to be unbiased and i.i.d. with the standard deviation σ. Then, using Eq. (22), the estimates of the desired parameters can be presented as

$$\Delta\hat{\boldsymbol{\pi}} = \Delta\boldsymbol{\pi} + \left(\sum_{i=1}^{m}\sum_{j=1}^{n} \mathrm{J}_{\pi i}^{j(p)T}\mathrm{J}_{\pi i}^{j(p)}\right)^{-1}\left(\sum_{i=1}^{m}\sum_{j=1}^{n} \mathrm{J}_{\pi i}^{j(p)T}\boldsymbol{\varepsilon}_i^j\right) \tag{26}$$

where the second term describes the stochastic component. As follows from this expression, the considered identification algorithm provides the unbiased estimate of the desired parameters, i.e., $E(\Delta\hat{\boldsymbol{\pi}}) = \Delta\boldsymbol{\pi}$ where, $E(\cdot)$ denotes the mathematical expectation of the random value. Taking into account the statistical properties of the measurement errors (which are assumed to be similar for all reference points, all manipulator configurations and all directions, in accordance with expression $E\left(\boldsymbol{\varepsilon}_i\boldsymbol{\varepsilon}_i^T\right) = \sigma^2\mathrm{I}$), the desired covariance matrix of $\Delta\boldsymbol{\pi}$, which defines the identification accuracy, can be computed as

$$\mathrm{cov}(\Delta\hat{\boldsymbol{\pi}}) = \sigma^2\left(\sum_{i=1}^{m}\sum_{j=1}^{n} \mathrm{J}_{\pi i}^{j(p)T}\mathrm{J}_{\pi i}^{j(p)}\right)^{-1} \tag{27}$$

Hence, the impact of the measurement errors on the identified values of the geometric parameters is defined by the matrix sum $\sum_{i=1}^{m}\sum_{j=1}^{n} \mathrm{J}_{\pi i}^{j(p)T}\mathrm{J}_{\pi i}^{j(p)}$ that in literature is also called the information matrix. It is clear that to achieve the best accuracy, the elements of covariance matrix (27) should be as small as possible. This requirement can be satisfied by proper selection of the experiment input data (i.e., the measurement configurations $\{\mathrm{q}_i,\ i = \overline{1, m}\}$) as well as by increasing the number of experiments m. Since increasing of the measurements is rather time consuming, it is reasonable to investigate the first approach that deals with optimization of the measurement configurations for limited number of experiments.

In more general case when the measurement errors differ from direction to direction, the expectation $E\left(\boldsymbol{\varepsilon}_i\boldsymbol{\varepsilon}_i^T\right)$ can be expressed as

$$E\left(\boldsymbol{\varepsilon}_i^j\boldsymbol{\varepsilon}_k^{jT}\right) = diag\left(\sigma_{xi}^{j2},\ \sigma_{yi}^{j2},\ \sigma_{zi}^{j2}\right),\ \text{if } i = k \tag{28}$$

(see our previous study on this issue presented in [54]). So, the covariance matrix defining the calibration accuracy can be rewritten in the following form

$$\mathrm{cov}(\Delta\hat{\boldsymbol{\pi}}) = \sigma^2\left(\sum_{i=1}^{m}\sum_{j=1}^{n} \mathrm{J}_{\pi i}^{j(p)T}\mathrm{W}_i^{j2}\mathrm{J}_{\pi i}^{j(p)}\right)^{-1} \tag{29}$$

where the weighting coefficient matrix W_i^j can be computed as in Eq. (24). It is clear that here the optimization of measurement configurations is also promising. However, in practice for the design of calibration experiments, the measurement errors are assumed to follow the i.i.d assumption.

In the literature, the problem of optimal pose selection for calibration experiments have been studied in a number of works [36,39–44], where several scalar criteria were proposed to defined this type of optimality in formal way. The main drawback of these approaches is that the relevant optimization objectives are not directly related to the manipulator positioning accuracy and its targeted industrial application (they usually focus on the parameter identification accuracy). Hence, in order to achieve simultaneously high accuracy both for the manipulator parameters and for the end-effector position (or to find reasonable trade-off), it is required to revise the existing techniques and to define a proper objective for measurement pose selection, taking into account the specificities of the application area studied in this work. This issue is in the focus of the next section.

6. Optimal selection of measurement configurations

This section proposes a new approach for calibration experiments design that has two distinct features: (i) optimization based on a new industrial-oriented performance measure that evaluates the manipulator positioning accuracy after calibration; (ii) utilization of experimental data obtained by means of the enhanced partial pose measurement method.

6.1. Test-pose based approach for calibration experiments design

In robot calibration, the desired manipulator parameters are estimated using experimental data corrupted by the measurement noise. For this reason, the parameters estimates are not equal to the true values, they vary from one set of experiments to another and can be treated as random ones. As follows from previous section, relevant identification algorithms provide unbiased estimates (i.e. their expectation is equal to the true values) but their dispersion essentially depends on the set of measurement configurations that provides the experimental data for the identification. Hence, it is reasonable to select the measurement configurations in the best way, in order to ensure the lowest impact of the measurement errors on the parameter estimates. In the literature, this problem is known as the "calibration experiments design". However, existing approaches focus on the *accuracy of the parameter estimation* (defined by the relevant covariance matrix (27)), while the considered industrial application motivates us to focus on the *manipulator positioning accuracy* after calibration.

In more details, the notion of manipulator positioning accuracy after calibration is illustrated in Fig. 6. It is assumed here that the

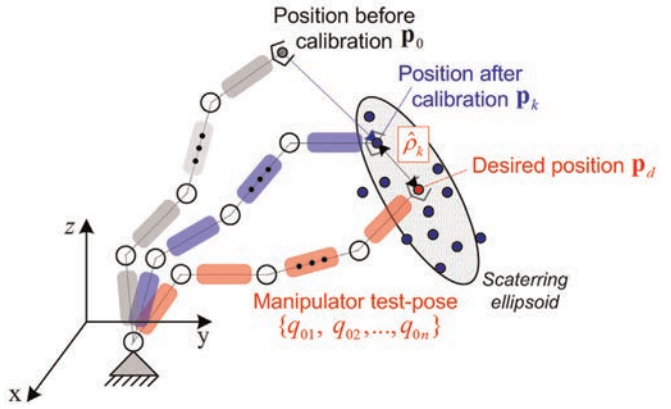

Fig. 6. Dispersion of the manipulator positioning errors after calibration and performance measure for selection of measurement configurations (for given single target point).

desired end-effector position is p_d, but without calibration, the end-effector is located at the point $\mathrm{p}_0 = g(\mathrm{q}_0, \boldsymbol{\pi})$, which can be computed using the nominal geometric model. Here, the joint coordinate vector q_0 is obtained from equation $\mathrm{p}_d = g(\mathrm{q}_0, \boldsymbol{\pi}_0)$ via the inverse kinematics. Using calibration, for each set of experimental data, it is possible to find the parameter estimates $\hat{\boldsymbol{\pi}}_k$ that allow us to compensate partially the positioning errors by computing another joint coordinate vector q_k from the equation $\mathrm{p}_d = g(\mathrm{q}_k, \hat{\boldsymbol{\pi}}_k)$ and to relocate the end-effector at the point $\mathrm{p}_k = g(\mathrm{q}_k, \boldsymbol{\pi})$, which is closer to the desired position p_d. Evaluating the distribution of Cartersian coordinates of points p_k, it should be mentioned that those points are concentrated around the desired position p_d in such way that:

$$E(\mathrm{p}_k) = \mathrm{p}_d \tag{30}$$

So, the target position can be treated as the center. To evaluate their dispersion with respect to the desired position, relevant distances $\rho_k = \mathrm{dist}(\mathrm{p}_k, \mathrm{p}_d)$ can be used. This leads to the following statistical performance measure

$$\rho_0 = \sqrt{E\left((\mathrm{p}_k - \mathrm{p}_d)^T(\mathrm{p}_k - \mathrm{p}_d)\right)} \tag{31}$$

which is the root-mean-square distance between the target position and the end-effector position after calibration. This indicator is used below to describe the geometric errors compensation efficiency. It is clear that the performance measure ρ_0 is directly related to the manipulator accuracy in an engineering viewpoint.

It is clear that the positioning error scattering and relevant performance measure ρ_0 highly depend on the target point position and varies throughout the workspace. In the frame of this work, it is assumed that the manipulator accuracy can be evaluated for so-called *test-pose* that is specified in the relevant technological process. This idea allows us to use the above mentioned performance measure ρ_0 as an objective in the calibration experiments design.

Using the adopted notations and assuming that the manipulator geometric model is linearized, the distance ρ_k can be computed as the Euclidean norm of the vector $\delta\mathrm{p}_k = \mathrm{J}_{\pi 0}^{(p)}\delta\boldsymbol{\pi}_k$, where the subscript'0' in the identification Jacobian $\mathrm{J}_{\pi 0}^{(p)}$ is related to the test pose q_0 and $\delta\boldsymbol{\pi}_k = \hat{\boldsymbol{\pi}}_k - \boldsymbol{\pi}$ is the difference between the estimated and true values of the robot geometric parameters respectively. Further, taking into account expression (26) and the assumptions concerning the measurement errors that are treated as unbiased and i.i.d. random variables, it can be easily proved that the expectation $E(\delta\mathrm{p}_k) = 0$. Therefore, the points p_k that the end-effector attains after compensation are located around the desired position p_d, as shown in Fig. 6.

The dispersion of these points can be evaluated by the variance $E\left(\delta\mathrm{p}_k{}^T\delta\mathrm{p}_k\right)$ which in accordance with the above definition is equal to the square of the performance measure ρ_0. This yields the following expression

$$\rho_0^2 = E\left(\delta\boldsymbol{\pi}^T\mathrm{J}_{\pi 0}^{(p)T}\mathrm{J}_{\pi 0}^{(p)}\delta\boldsymbol{\pi}\right) \tag{32}$$

which can be rewritten using the identity equation $\delta\mathrm{p}^T\delta\,\mathrm{p} \equiv \mathrm{trace}(\delta\mathrm{p}\delta\mathrm{p}^T)$ as

$$\rho_0^2 = \mathrm{trace}\left(\mathrm{J}_{\pi 0}^{(p)}E(\delta\boldsymbol{\pi}\delta\boldsymbol{\pi}^T)\mathrm{J}_{\pi 0}^{(p)T}\right) \tag{33}$$

Further, by applying Eq. (27) and considering that the term $E(\delta\boldsymbol{\pi}\delta\boldsymbol{\pi}^T)$ is the covariance matrix of the geometrical error estimates, i.e., $E(\delta\boldsymbol{\pi}\delta\boldsymbol{\pi}^T) = \mathrm{cov}(\hat{\boldsymbol{\pi}})$, the desired expression can be presented in the final form as

$$\rho_0^2 = \sigma^2\cdot\mathrm{trace}\left(\mathrm{J}_{\pi 0}^{(p)}\left(\sum_{i=1}^{m}\sum_{j=1}^{n}\mathrm{J}_{\pi i}^{j(p)T}\mathrm{J}_{\pi i}^{j(p)}\right)^{-1}\mathrm{J}_{\pi 0}^{(p)T}\right) \tag{34}$$

As follows from this expression, ρ_0^2 can be treated as the *weighted trace of the covariance matrix* $\mathrm{cov}(\hat{\boldsymbol{\pi}})$, where the weighting coefficients are computed using the test-pose joint coordinates q_0. Hence, the proposed performance measure has obvious advantage compared to the existing ones [40], which operate with "pure" trace of this matrix and involve straightforward summing of its diagonal elements (which may be of different units). Based on this performance measure, the calibration experiments design can be reduced to the following optimization problem

$$\mathrm{trace}\left(\mathrm{J}_{\pi 0}^{(p)}\left(\sum_{i=1}^{m}\sum_{j=1}^{n}\mathrm{J}_{\pi i}^{j(p)T}\mathrm{J}_{\pi i}^{j(p)}\right)^{-1}\mathrm{J}_{\pi 0}^{(p)T}\right) \to \min_{\{\mathrm{qi}\ldots\mathrm{qm}\}} \tag{35}$$

whose solution gives a set of the desired measurement configurations $\{\mathrm{q}_1, \ldots, \mathrm{q}_m\}$.

Hence, in the frame of the proposed approach, the calibration quality (evaluated via the error compensation accuracy ρ_0) is completely defined by the set of Jacobian matrices $\left\{\mathrm{J}_{\pi 1}^{(p)}, \ldots, \mathrm{J}_{\pi m}^{(p)}\right\}$ that depend on the manipulator configurations $\{\mathrm{q}_1, \ldots, \mathrm{q}_m\}$, while the Jacobian matrix $\mathrm{J}_{\pi 0}^{(p)}$ corresponding the test-pose q_0 defines the weighting coefficients. It is worth mentioning that test-pose based approach can be also extended for calibration of the manipulator elasto-static parameters (see [55], for more details). The advantages of the proposed approach will be illustrated in the following subsections.

6.2. Comparison analysis of the proposed and conventional approaches

Let us illustrate the advantages of the test-pose based approach by an example of the geometrical calibration of a two-link planar manipulator. It is assumed that the nominal link lengths $\{l_1, l_2\}$ differ from the real ones, and these deviations $\{\Delta l_1, \Delta l_2\}$ should be identified by means of calibration. In this case, the manipulator end-effector position can be expressed as

$$\begin{aligned} p_x &= (l_1 + \Delta l_1)\cos\ q_1 + (l_2 + \Delta l_2)\cos(q_1 + q_2) \\ p_y &= (l_1 + \Delta l_1)\sin\ q_1 + (l_2 + \Delta l_2)\sin(q_1 + q_2) \end{aligned} \tag{36}$$

where p_x and p_y define the end-effector position, q_1, q_2 are the joint coordinates that define the manipulator configuration. It can be proved that in this case the parameter covariance matrix does not depend on the angles q_{1i} and is expressed as

$$\mathrm{cov}(\Delta\boldsymbol{\pi}) = \frac{\sigma^2}{m^2 - \left(\sum_{i=1}^{m} \cos\ q_{2i}\right)^2} \begin{bmatrix} m & -\sum_{i=1}^{m} \cos\ q_{2i} \\ -\sum_{i=1}^{m} \cos\ q_{2i} & m \end{bmatrix} \quad (37)$$

where the vector $\Delta\boldsymbol{\pi} = (\Delta l_1, \Delta l_2)$ denotes the parameters deviations to be identified, m is the number of experiments and σ is the standard deviation. of the measurement noise.

For comparison purposes, the plans of experiments were obtained using three different strategies:

(1) the measurement configurations were generated randomly;
(2) the measurement configurations were obtained using the conventional approach based on D-optimality principle;
(3) the measurement configurations were obtained using the proposed test-pose based approach (see Section 6.1).

For the first approach (i), the measurement configurations were found in a trivial way, using a uniform random number generator scaled within the joint limits. For the conventional approach (ii), where the D-optimality principle was used (that has been proved to be efficient in many applications), the performance measure is equal of the covariance matrix determinant (37), which yields

$$\det(\mathrm{cov}(\Delta\boldsymbol{\pi})) = \frac{\sigma^2}{m^2 - \left(\sum_{i=1}^{m} \cos\ q_{2i}\right)^2} \quad (38)$$

As follows from this expression, this criterion requires minimization of the term $(\sum_{i=1}^{m} \cos\ q_{2i})^2$. So, the determinant minimum value is equal to σ^2/m^2 and it is reached when

$$\sum_{i=1}^{m} \cos\ q_{2i} = 0,\ i = 1, \dots, m \quad (39)$$

It should be mentioned that this optimality condition also satisfies the A- and G-optimality principles. More details concerning the calibration experiment planning using the above conditions can be found in [56].

For the proposed approach (iii), it is assumed that the calibration quality is evaluated in the predefined manipulator test configuration (q_{10}, q_{20}). In this case, the performance measure ρ_0^2 (34) can be computed as

$$\rho_0^2 = 2\sigma^2 \cdot \frac{m - \cos\ q_{20} \sum_{i=1}^{m} \cos\ q_{2i}}{m^2 - \left(\sum_{i=1}^{m} \cos\ q_{2i}\right)^2} \quad (40)$$

As follows from relevant analysis, the minimum value of ρ_0^2 is equal to

$$\rho_{0\ \min}^2 = \frac{\sigma^2}{m} \cdot \frac{\cos^2 q_{20}}{1 - |\sin\ q_{20}|} \quad (41)$$

and it is achieved when the measurement configurations satisfy the equation

$$\sum_{i=1}^{m} \cos\ q_{2i} = m \cdot \frac{1 - |\sin\ q_{20}|}{\cos\ q_{20}} \quad (42)$$

which essentially differ from (39). It should be mentioned that general solution of Eq. (42) for m configurations can be replaced by the decomposition of the whole configuration set by the subsets of 2 and 3 configurations (while providing the same identification accuracy). This essentially reduces computational complexity and allows user to reduce number of different measurement configurations without loss of accuracy.

Table 2
Accuracy comparison of the proposed and conventional approaches

Test-pose (q_{20}), [deg.]	0	30	60	90	120	150	180
ρ_0^2/ρ_c^2	0.5	0.75	0.83	1	0.83	0.75	0.5
Accuracy improvement (%)	41	15	10	0	10	15	41

Using the above presented expressions for the robot accuracy after calibration, the proposed and conventional approaches can be compared analytically and numerically. In particular, for the test pose $(*, q_{20})$, the conventional approach (ii) ensures the positioning accuracy after compensation $\rho_c^2 = 2\sigma^2/m$, while for the proposed approach (iii), similar performance measure is equal to $\rho_{0\ \min}^2 = \sigma^2/m \cdot \cos^2 q_{20}/(1 - |\sin\ q_{20}|)$. Corresponding values are compared in Table 2, which proves that using the proposed approach for the calibration experiment design allows us to improve the positioning accuracy up to 41%.

To illustrate advantages of the proposed approach, Fig. 7 presents simulation results for manipulator positioning errors after compensation corresponding to three different sets of measurement configurations employed in calibration. It is also assumed that the manipulator parameters are $l_1 = 1$ m, $l_2 = 0.8$ m; the number of measurement configurations $m = 2$; the test configuration is defined by the vector $\mathrm{q}_0 = (-45^\circ,\ 20^\circ)$, and the s.t.d. of the measurement errors is $\sigma = 1$ mm. For comparison purposes, the following plans of experiments (measurement configurations) have been considered:

(1) **Random plan:** $\mathrm{q}_1 = (0^\circ,\ -10^\circ)$ and $\mathrm{q}_2 = (0^\circ,\ 10^\circ)$, which has been generated randomly;
(2) **Conventional plan**: $\mathrm{q}_1 = (0^\circ,\ -90^\circ)$ and $\mathrm{q}_2 = (0^\circ,\ 90^\circ)$, which satisfies D-optimality principle [34];
(3) **Proposed plan**: $\mathrm{q}_1 = (0^\circ,\ -46^\circ)$ and $\mathrm{q}_2 = (0^\circ,\ 46^\circ)$, which satisfies the test-pose based approach.

To obtained reliable statistics, the calibration experiments have been repeated 100 times. Corresponding results presented in Fig. 7 show that the proposed approach allows us to increase accuracy of the end-effector position on average by 18% comparing to the D-optimal plan and by 48% comparing to the randomly generated plan.

Hence, this simple example confirms that the proposed performance measure is attractive for practicing engineers and allows us to avoid the multi-objective optimization problem that arises while minimizing all elements of the covariance matrix (27) simultaneously. In addition, using this approach, it is possible to find a balance between the accuracy of different geometrical parameters whose influence on the final robot accuracy is unequal. Another example confirming this conclusion is presented in our previous work [57].

It is worth mentioning that the proposed approach allows essential improvement of the calibration efficiency and to achieve the best manipulator positioning accuracy for the user-defined test configurations related to the manufacturing task (in contrast to the conventional approaches that are targeted at the best parameter identification accuracy). However, for typical industrial robots whose model includes very high number of parameters, relevant optimization becomes extremely time consuming. For this reason, the next subsection focuses on simplification of numerical routines employed in the selection of optimal measurement configurations.

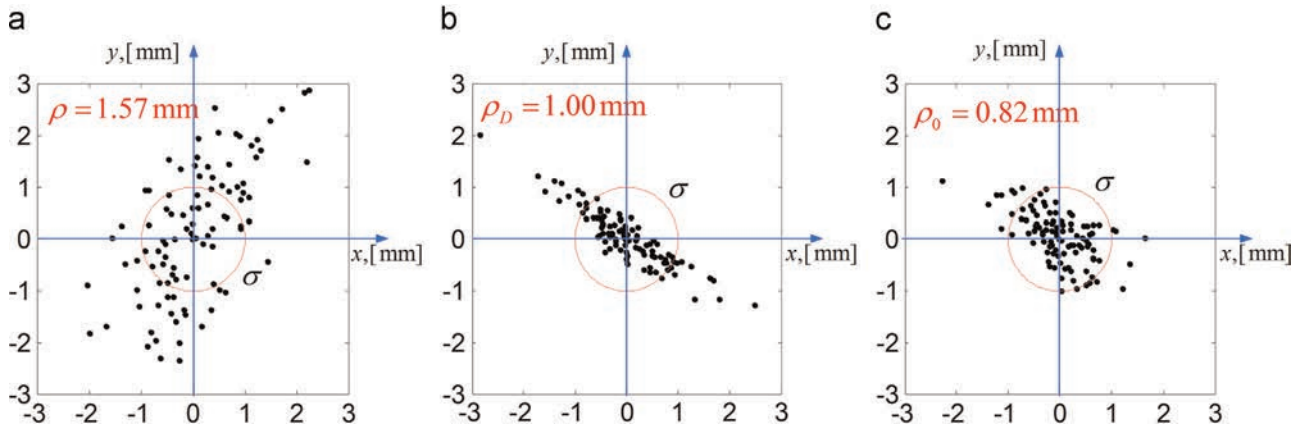

Fig. 7. Dispersion of manipulator positioning errors after calibration for different plans of experiments: (a) Random plan, (b) conventional plan and (c) proposed plan.

6.3. Simplification of the optimal pose selection procedure

It is clear that analytical solutions of relevant optimization problems (35) can hardly be obtained (for example, when the number of parameters to be identified is very high, the analytical computations of the matrix inversion in these expressions are hardly possible). So, applying a numerical optimization technique is the only reasonable way, but the convergence rate, the total computational time and ability to attain the global minimum become key issues. For this reason, several conventional optimization techniques were examined. In order to improve their efficiency, two techniques that are adapted to the test-pose based approach have been proposed: (i) application of parallel and hybrid computations; (ii) generation of quasi-optimal solutions using lower-dimensional calibration plans.

In order to obtain the global optimum for the considered problem, it is required numerous repetitions of the optimization with different starting points. As follows from our experiences, even using thousands of them may be not enough for finding the global optimum but the required computational time could overcome hundreds of hours. So, it is reasonable to apply *parallel computing* technique to speed up the design process and to take advantage of multi-core architecture in modern computers. Relevant computations in this work were carried out on a workstation with 12 cores, which allowed us to decrease the computational time by the factor of 10–12. However, it is not enough yet to solve the problem of real industrial size, where several dozen of parameters should be identified. To overcome this difficulty, it has been proposed a hybrid approach that combines advantages of the genetic algorithm and the gradient search. The idea behind this technique is to modify the starting point selection strategy for the gradient search in order to improve the algorithm efficiency. To ensure better convergence to the global minimum, it has been proposed to use the best half of final solutions obtained from GA as the starting points for gradient search. This hybrid approach has been proved to be quite efficient in terms of computational time (improved by a factor of 5, in addition to parallel computing) and allows us to avoid convergence to the local minima.

On the other hand, as follows from our experiences, the diversity of the measurement poses does not contribute significantly to the accuracy improvement if m (the total number of measurements) is high enough. This allows us to propose an *alternative technique*, which uses the same measurement configurations several times (allowing to simplify and speed up the measurements). This approach can be also referred to as the "reduction of problem dimension".

To explain the proposed approach in more details, let us assume that the problem of the optimal pose selection has been solved for m different configurations and the obtained calibration plan ensures the positioning accuracy ρ_0^m. Using these notations, let us evaluate the calibration accuracy for two alternative strategies that employ total number of experiments $k \times m$:

Strategy #1 (*conventional*): the measurement configurations are found from the full-scale optimization of size $k \times m$.

Strategy #2 (*proposed*): the measurement configurations are obtained by simple repetition of the configurations got from the low-dimensional optimization problem of size m (i.e. at each configuration, the measurements are repeated k times).

It is clear that the calibration accuracy ρ_0^{km} for the strategy #1 is better than the accuracy corresponding to the strategy #2 that can be expressed as $\rho_0^m/\sqrt{k}$. However, as follows from our study, this difference is quite small if the total number of measurements is high enough, while the number of different configurations m is larger than 3. This allows us to essentially reduce the size of the optimization problem employed in the optimal selection of measurement poses without significant impact on the positioning accuracy.

To demonstrate the validity of the proposed approach, a benchmark example that deals with geometric calibration of a 6-dof manipulator has been solved using strategies #1 and #2, assuming that the total number of measurements is equal to 12 (i.e. using different factorizations such as 12×1, 6×2, 4×3, 3×4). Relevant results are presented in Table 3, where the first four lines give the accuracy ρ_0 and the last line shows corresponding computational time. It is noteworthy that the factorization 12×1, where all measurement poses are different, is only 6% better comparing to the factorization 3×4 where measurements are repeated 4 times in 3 different configurations. At the same time, the factorizations 6×2 and 4×3 give almost the same results as the factorization 12×1. On the other hand, the computational time of the optimal pose generation for $m = 3$ is much lower than for $m = 12$. Hence, as follows from these results, repeating experiments with optimal plans obtained for the lower number of configurations provides almost the same performance as "full-dimensional" optimal plan. Obviously, this reduction of the measurement pose number is very attractive from an engineering viewpoint. This technique will be used in the application example presented in the following section.

7. Experimental results: geometric calibration of KUKA KR-270

To confirm the applicability of the proposed calibration techniques and demonstrate their benefits from engineering point of view, this section presents the experimental procedure, the identification results as well as the accuracy analysis for geometric

Table 3
Comparison of the optimal and quasi-optimal solutions for measurement configurations in calibration experiments, evaluated via $\rho_0^{\min}$, [mm] (case of a 6-dof manipulator, repetitions of measurements k times for m different configurations)

Total number of measurements	Number of different configurations			
	$m = 3$	$m = 4$	$m = 6$	$m = 12$
$km = 3$	0.0637 (3 × 1)			
$km = 4$		0.0521 (4 × 1)		
$km = 6$	0.0450 (3 × 2)		0.0426 (6 × 1)	
$km = 12$	0.0319 (3 × 4)	0.0301 (4 × 3)	0.0301 (6 × 2)	0.0301 (12 × 1)
Computational time	38 min	45 min	56 min	1.6 h

calibration of the industrial KUKA KR-270 robot.

7.1. Experimental environment and measurement setup

The manufacturing cell where the examined robot has been installed is presented in Fig. 8. The work-cell includes a 6-dof industrial KUKA KR-270 robot with six revolute joints, a machining table, a vertical frame for mounting the pieces. It should be noted that for geometric calibration, the above mentioned equipment (that can be also treated as the obstacles) cause some limits for placement of the external measurement device. Taking into account particularities of the technological process considered in this work, the manipulator test-pose (configurationq_0) has been defined in the location where the best robot positioning accuracy should be achieved: $q_0 = (76.7^\circ, -56.9^\circ, 89.3^\circ, 45.1^\circ, 76^\circ, 57.2^\circ)$. It is worth mentioning that similar configuration has been used in previous works [58,59] to evaluate the quality of the robot-based machining.

To identify the desired geometric parameters, the manufacturing cell is equipped with some additional measuring devices that provide us with Cartesian coordinates of the references points for each manipulator configuration. Besides, the manipulator joint angles required for the identification procedure are obtained from the robot control system. So, entire experimental setup includes the following units:

- 6-dof KUKA KR-270 robotic manipulator whose geometric parameters should be identified (repeatability of this robot is 60 μm [60], details concerning its kinematics are presented in Section 3);
- Robot control system KR-C2, which is used for changing the manipulator configurations and measuring the corresponding joint angles with a precision equal to $\pm 0.0001^\circ$;
- Special measurement tool with three reference points located on the circle of radius 104 mm, this tool is attached to the manipulator mounting flange;
- Laser tracker Leica AT-901 that is used to measure the Cartesian coordinates of the reference point with a precision of 10 μm [61];
- Laser tracker reflector that is sequentially attached to the reference points (with precision about 1 μm), it allows the measurement device to estimate the distances and compute the required Cartesian coordinates;

The experimental setup for manipulator geometric calibration is shown in Fig. 9. It is worth mentioning that the calibration experiments are carried out in a limited area (smaller than the robot entire workspace) caused by the work-cell size limitation and some obstacles. For this reason, some of the manipulator configurations cannot be reached during the experiments (As a consequence, they are not included in the optimal plan).

7.2. Optimal measurement pose selection

While selecting the minimum number of measurement configurations, it is necessary to keep in mind that each manipulator pose produces 6 independent equations only that are used for identification. On the other hand, the set of geometric parameters to be identified includes 33 unknowns:

(1) 18 principal parameters of the KUKA KR-270 robot;
(2) 6 parameters describing the laser tracker location with respect to the robot base frame (both position and orientation);
(3) 9 parameters describing locations of the end-effector reference points with respect to the manipulator mounting flange (positions only for three points).

Therefore, at least six different measurement configurations are required to ensure non-singularity of the identification Jacobian and ability to estimate the desired values. For this reason, relevant optimization problem aiming at determining optimal measurement poses has been solved for the configuration number $m = 6$.

To take into account the manipulator joint limits and the work-cell constraints, the optimization problem for measurement

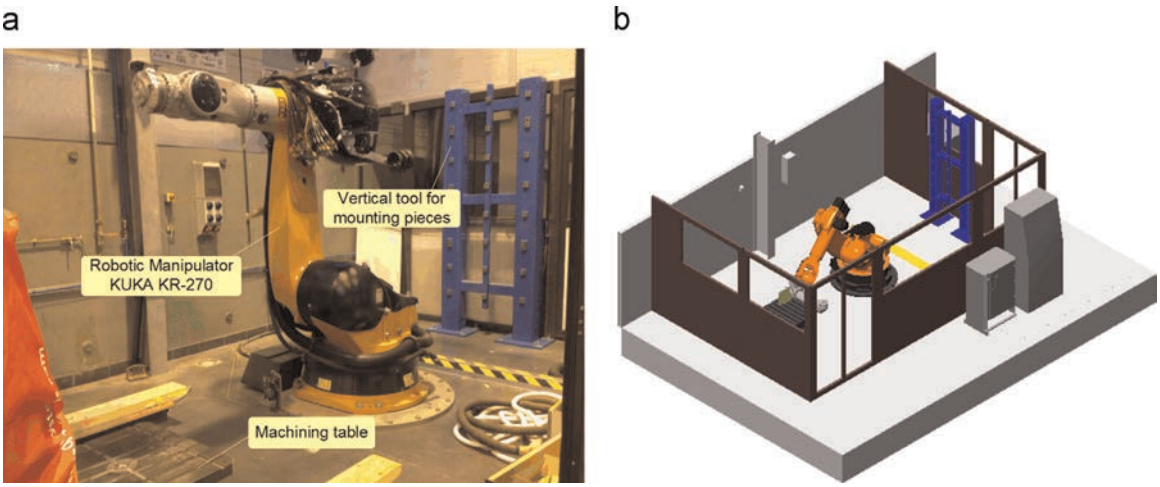

Fig. 8. The experimental work-cell environment: (a) general view; (b) typical machining configuration (test-pose).

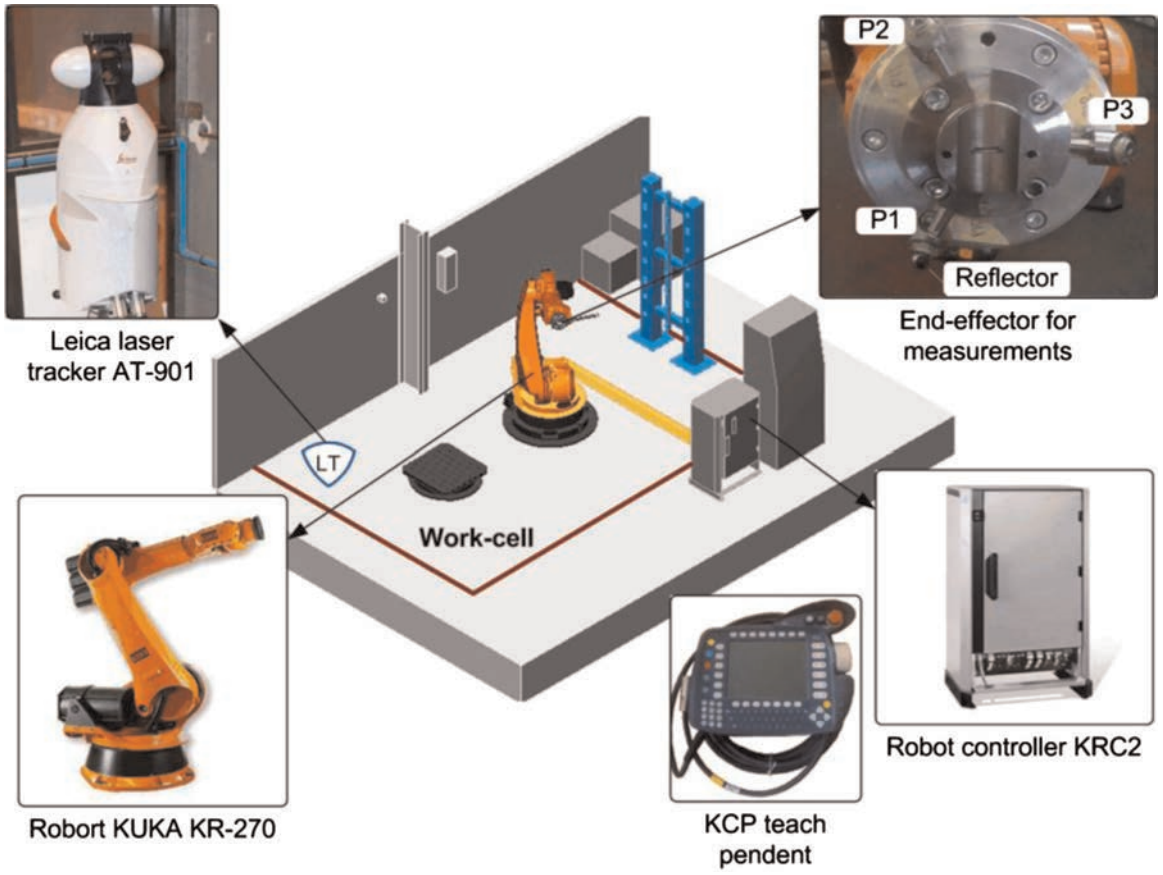

Fig. 9. Experimental setup for manipulator geometric calibration.

Table 4
The joint limits of robot KUKA KR-270

	q_1	q_2	q_3	q_4	q_5	q_6
q^{min}, [deg.]	−180	−145	−110	−180	−125	−180
q^{max}, [deg.]	180	0	155	180	125	180

Table 5
The work-cell space boundaries with respect to the robot base frame

	p_x	p_y	p_z
p^{min}, [mm]	−1400	−3000	300
p^{max}, [mm]	1800	2200	3500

configurations selection (see Eq.(35)) should be solved subject to $q^{min} \le q_i \le q^{max}$ and $p^{min} \le g(q_i) \le p^{max}$. In particular, $\{q_i i = \overline{1,6}\}$ denote the measurement configurations, the function $g(q_i)$ describes the manipulator geometric model and returns the end-effector position coordinates of the current configuration. These constraints take into account the manipulator joint limits [q^{min}, q^{max}] and the work-cell boundaries [p^{min}, p^{max}], whose values are given in Table 4 and 0, respectively. Table 5

This optimization problem has been solved using the MATLAB software with the built-in optimization functions “ga” and “fmincon”, which are required for the proposed hybrid approach that employs the genetic algorithm and the gradient search. Corresponding solution minimizes the objective function ρ_0 (the

Table 6
Comparison of calibration plans with different diversity of measurement configurations.

Calibration plans		Robot accuracy ρ_0, [μm]	Computational time
(*i*)	{Sol. #1×3}	7.85	56 min
	{Sol. #2×3}	7.84	56 min
	{Sol. #3×3}	7.83	56 min
(*ii*)	{Sol. #1×2, Sol. #2}	7.84	1.9 h
	{Sol. #1×2, Sol. #3}	7.84	1.9 h
	{Sol. #1, Sol. #2×2}	7.83	1.9 h
	{Sol. #2×2, Sol. #3}	7.83	1.9 h
	{Sol. #1, Sol. #3×2}	7.83	1.9 h
	{Sol. #2, Sol. #3×2}	7.83	1.9 h
(iii)	{Sol. #1, Sol. #2, Sol. #3}	7.83	2.8 h
	Random configurations (for comparison)	17.33	~0.05 s

Table 7
Identification results for manipulator tool transformations

	Reference point #1 (P1)		Reference point #2 (P2)		Reference point #3 (P3)	
	Value, [mm]	CI	Value, [mm]	CI	Value, [mm]	CI
p_x	277.23	±0.05	276.49	±0.05	278.44	±0.05
p_y	−46.53	±0.04	−48.25	±0.04	103.73	±0.05
p_z	−93.87	±0.04	94.05	±0.05	−2.17	±0.05

Table 8
Identification results for manipulator geometric parameters

Parameter	Unit	Value	Confidence interval	
			Estimated using covariance matrix	Estimated using Gibbs sampling
$p_{x1} \equiv \Delta d_2$	[mm]	−0.353	±0.086	±0.102
p_{y1}	[mm]	0.426	±0.272	±0.421
φ_{x1}	[deg.]	0.015	±0.005	±0.005
Δq_2	[deg.]	−0.007	±0.005	±0.004
$p_{x2} \equiv \Delta d_3$	[mm]	0.458	±0.082	±0.060
φ_{x2}	[deg.]	0.022	±0.014	±0.022
φ_{z2}	[deg.]	−0.023	±0.005	±0.005
Δq_3	[deg.]	−0.023	±0.019	±0.013
$p_{x3} \equiv \Delta d_4$	[mm]	−0.214	±0.089	±0.093
$p_{z3} \equiv \Delta d_5$	[mm]	−0.508	±0.363	±0.259
φ_{z3}	[deg.]	−0.011	±0.017	±0.022
Δq_4	[deg.]	0.001	±0.008	±0.009
p_{y4}	[mm]	−0.167	±0.113	±0.044
p_{z4}	[mm]	−0.018	±0.073	±0.044
φ_{z4}	[deg.]	0.025	±0.015	±0.010
Δq_5	[deg.]	−0.011	±0.027	±0.009
p_{z5}	[mm]	0.016	±0.104	±0.041
φ_{z5}	[deg.]	−0.008	±0.018	±0.007

Table 9
Evaluation of the manipulator accuracy improvement based on residual analysis

Criterion		Before calibration	After calibration	Improvement factor
Coordinate-based residuals, [mm]	max	1.25	0.32	4.0
	RMS	0.54	0.10	5.3
Distance-based residuals, [mm]	max	1.31	0.39	3.5
	RMS	0.94	0.17	5.5

proposed performance measure), which describes the manipulator positioning accuracy after calibration. The measurement noise parameter σ has been taken from the technical specification of the laser tracker and is equal to 10 μm. It should be mentioned that, in order to reduce the computational efforts and, to pay more attention to the parameters that can be tuned in the robot controller, only nine the most essential geometric parameters were considered while computing the Jacobian matrices $\mathbf{J}_{\pi 0}^{(p)}$ and $\mathbf{J}_{\pi i}^{(p)}$. They include the link lengths $\{d_2, \dots, d_5\}$ whose nominal values are known and the joint offsets $\{\Delta q_1, \dots, \Delta q_5\}$ that are nominally equal to zero.

In order to find a solution as close as possible to the global minimum, the optimization problem has been solved several times with different starting points. Nevertheless, three different solutions have been obtained that ensure almost the same value of the considered performance measure ρ_0 (≈13.6μm). Corresponding solutions (measurement configurations) are presented in [45]. For comparison purposes, these solutions have been evaluated both separately and in different combinations, assuming that the measurements are performed 18 times in the following way: (*i*) repeating three times the measurements in configurations from a single set; (*ii*) using twice configurations from one set and only once from the second set; (*iii*) using all configurations from three sets simultaneously (but only once). Corresponding values of ρ_0 are presented in Table 6. As follows from this table, the diversity of manipulator configurations has almost negligible contribution to the improvement of robot accuracy (it is about 7.85 μm, the difference is less than 0.2%). This confirms the results from Subsection 6.3, which claims that using simple repetition of the optimal plan with lower number of measurement configurations essentially reduces the experimental complexity while the same calibration accuracy can be achieved.

7.3. Identification of geometric parameters

The obtained measurement configurations have been used for the calibration experiments for KUKA KR-270 industrial robot. It is worth mentioning that each manipulator configuration provides 27 values of the position coordinates. These coordinates have been obtained using *two different locations of the laser tracker* (see more details in [45]). However, at certain configurations, some of the reference points were not visible for both laser tracker locations. This problem can be solved by increasing the number of laser tracker locations, but in practice such solution is limited by the experimental time as well as the work-cell constraints. On the other hand, since the calibration experiment employs two laser tracker placements, 6 additional parameters describing the second laser tracker location should be also identified. In total, the system of identification equations contains 432 expressions that can be used to identify the whole set of 39 geometric parameters. To achieve the highest identification accuracy, here it is proposed to use all measurements corresponding to 18 manipulator configurations simultaneously for calibration of the geometric parameters.

Using the obtained measurement data, the two-step identification procedure has been applied (see Section 5). On the first step, the base and tool transformations have been computed, corresponding results are presented in Table 7. On the second step, these transformations have been used for the identification of the manipulator geometric parameters, which are presented in Table 8. It should be mentioned that in order to increase the identification accuracy, this two-step procedure has been repeated iteratively (280 iterations, computing time was less than two

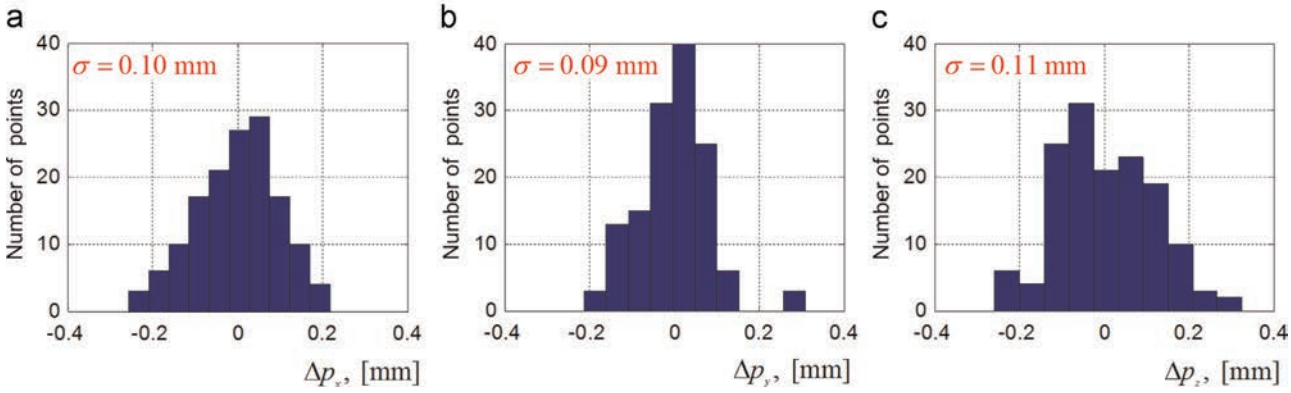

Fig. 10. Histograms of residual distribution along *X*-, *Y*-, and *Z*-directions after geometric calibration: (a) X-direction, (b) Y-direction and Z-direction.

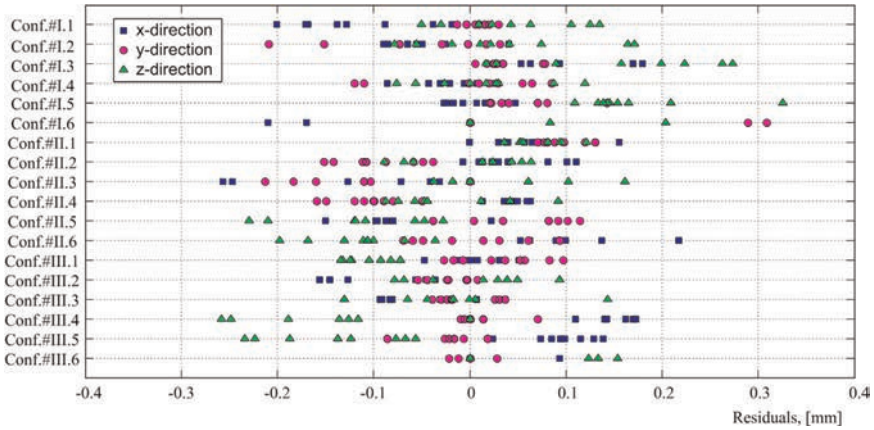

Fig. 11. Residual distribution after geometric calibration for different measurement configurations.

minutes). As follows from the results, the desired geometric parameters have been identified with high accuracy, which has been evaluated using two different techniques (based on the statistical properties extracted from the covariance matrix and using the Gibbs sampling).

The results presented in Table 8 include 18 parameters, some of which cannot be modified in the robot control software. So, it is useful to examine the effect of reducing the number of these parameters by setting them to their nominal values. Relevant analysis shows that the manipulator end-effector positioning error impact because of such a simplification essentially differs from one parameter to another, and they can be split into the following groups:

- Parameters $\{p_{x1}, p_{y1}, p_{x2}, p_{x3}, p_{z3}, p_{y4}, \Delta q_2, \Delta q_3, \varphi_{z2}, \varphi_{z3}, \varphi_{z4}\}$, whose neglecting leads to the loss of accuracy from 0.10 mm to 1.03 mm;
- Parameters $\{p_{z4}, p_{z5}, \Delta q_5, \varphi_{x1}, \varphi_{x2}, \varphi_{z5}\}$, whose neglecting leads to the loss of accuracy from 0.02 mm to 0.09 mm;
- Parameter Δq_4 , whose neglecting leads to the loss of accuracy is about 4 μm.

Comparing to the machining accuracy required for the considered milling process (0.05–0.25 mm), the above listed positioning error impacts are not negligible for the most of the geometric parameters. So, their deviations should be compensated either in the geometric model embedded in the robot controller or at the step of generation of the machining trajectory.

For comparison purposes, the manipulator accuracy improvement due to calibration has been studied based on the residual analysis before and after calibration (computed using the nominal and identified values of geometric parameters respectively). Here, two types of residuals have been examined, the coordinate-based and distance-based ones. Corresponding results are presented in Table 9, which includes the maximum and root mean square (RMS) values of the relevant residuals. As follows from the results, both types of the residuals have been essentially reduced after calibration. In particular, the maximum values have been reduced by a factor of 4 and 3.5, while the RMS values have been decreased by a factor of 5.3 and 5.5, respectively.

Hence, the obtained results allow us to improve essentially the manipulator accuracy for the measurement configurations that were used in the identification. So, it is reasonable to expect that using the geometric model, which integrates the identified parameters, the desired positioning accuracy for the given test configuration can be also achieved. A more detailed analysis concerning the parameter identification accuracy and its impact on the robot positioning accuracy are discussed in the next subsection.

7.4. Analysis of the identification results

In order to evaluate the calibration results, let us first analyze the residuals computed from the identification equations for each coordinate separately. Their histograms are shown in Fig. 10 and corresponding distributions for each configuration are presented in Fig. 11. As follows from the analysis, the residuals tend to follow the normal probability distributions with zero mean and almost the same parameter σ , which is equal to 0.10 mm, 0.09 mm, and 0.11 mm for *X*-, *Y*-, and *Z*- direction, respectively. The latter justifies the utilization of ordinary least square technique (with equal weights) for the parameter identification and allows us to conclude that the measurement noise parameter σ in our experiment is about 0.1 mm.

It is worth mentioning that the noise parameter σ estimated from the residual analysis is essentially higher than the precision of the laser tracker measurement system, which is defined in the technical specifications as 0.01 mm. This difference may be due to the limitations of the geometric model, which does not take into account a number of essential features such as the elastostatic deformations due to gravity forces, the friction/backlash in joints and other factors that affect the robot repeatability ($\pm$ 0.06 mm, as specified in the data sheets). Nevertheless, the geometric calibration ensures essential improvement of the robot accuracy in the unloaded mode. Relevant computations show that for the considered test-pose, it is possible to achieve a positioning accuracy of about 0.04 mm that is acceptable for the considered technological process. On the other hand, this issue motivates further research devoted to modeling of non-geometric factors and estimation of relevant parameters.

8. Conclusions

This paper presents a new approach for calibration experiments design for serial industrial robots. This approach employs a new industry-oriented performance measure, which evaluates the quality of calibration plan via the manipulator positioning accuracy after geometric error compensation, and considers the industrial requirements associated with the prescribed manufacturing task. It is proved that the proposed performance measure can be presented as the weighted trace of the relevant covariance matrix, where the weighting coefficients are defined by the corresponding test-pose. Such an approach allows us to find the

optimal measurement configurations for calibration experiments and to improve essentially the robot positioning accuracy for a desired manipulator test-pose.

Dedicated algorithm for geometric parameter identification is based on an enhanced partial pose measurement method, which uses only direct position measurements from an external device for several end-effector reference points. It allows the user to increase essentially the parameter identification accuracy and to avoid additional computations of the end-effector orientation components, which may cause non-homogeneity in relevant identification equations.

The obtained theoretical results have been validated via experimental study that deals with geometric calibration of a KUKA KR-270 industrial robot. The manipulator geometric parameters have been identified with accuracy equal to 0.15 mm and 0.01° for linear and angular ones respectively (in average). These results allowed us to achieve a manipulator positioning accuracy equals to 0.17 mm, which is 5.5 times better compared to the non-calibrated robot.

Acknowledgments

The authors would like to acknowledge the financial support of the French "Agence Nationale de la Recherche" (Project ANR-2010-SEGI-003-02-COROUSSO), France and FEDER ROBOTEX project, France.

References

[1] S. Aguado, D. Samper, J. Santolaria, J.J. Aguilar, Identification strategy of error parameter in volumetric error compensation of machine tool based on laser tracker measurements, Int. J. Mach. Tools Manuf. 53 (2012) 160–169.
[2] G. Du, P. Zhang, D. Li, Online robot calibration based on hybrid sensors using Kalman filters, Robot. Comput.-Integr. Manuf. 31 (2015) 91–100.
[3] A. Joubair, M. Slamani, I.A. Bonev, A novel XY-Theta precision table and a geometric procedure for its kinematic calibration, Robot. Comput.-Integr. Manuf. 28 (2012) 57–65.
[4] S. Marie, E. Courteille, P. Maurine, Elasto-geometrical modeling and calibration of robot manipulators: application to machining and forming applications, Mech. Mach. Theory 69 (2013) 13–43.
[5] A. Nubiola, I.A. Bonev, Absolute robot calibration with a single telescoping ballbar, Precis. Eng. 38 (2014) 472–480.
[6] Z.S. Roth, B. Mooring, B. Ravani, An overview of robot calibration, IEEE J. Robot. Autom. 3 (1987) 377–385.
[7] J. Santolaria, F.-J. Brosed, J. Velázquez, R. Jiménez, Self-alignment of on-board measurement sensors for robot kinematic calibration, Precis. Eng. 37 (2013) 699–710 7//.
[8] J. Santolaria, M. Ginés, Uncertainty estimation in robot kinematic calibration, Robot. Comput.-Integr. Manuf. 29 (2013) 370–384.
[9] A. Elatta, L.P. Gen, F.L. Zhi, Y. Daoyuan, L. Fei, An overview of robot calibration, Inform. Technol. J. 3 (2004) 74–78.
[10] A. Klimchik, A. Pashkevich, D. Chablat, G. Hovland, Compliance error compensation technique for parallel robots composed of non-perfect serial chains, Robot. Comput.-Integr. Manuf. 29 (2013) 385–393.
[11] D. Daney and I. Z. Emiris, Robust parallel robot calibration with partial information, in: Proceedings of the IEEE International Conference on, Robotics and Automation, ICRA, 2001, pp. 3262–3267.
[12] M.R. Driels, Full-pose calibration of a robot manipulator using a coordinate-measuring machine, Int. J. Adv. Manuf. Technol. 8 (1993) 34–41.
[13] M. Ikits and J. M. Hollerbach, Kinematic calibration using a plane constraint, in: Proceedings of the IEEE International Conference on Robotics and Automation, 1997, pp. 3191–3196.
[14] W. Veitschegger and C.-h. Wu, A method for calibrating and compensating robot kinematic errors, in: Proceedings of the IEEE International Conference on Robotics and Automation, 1987, pp. 39–44.
[15] H. Hage, P. Bidaud, and N. Jardin, Practical consideration on the identification of the kinematic parameters of the Stäubli TX90 robot, in: Proceedings of the 13th World Congress in Mechanism and Machine Science, Guanajuato, Mexico, 2011, p. 43.
[16] J.-M. Renders, E. Rossignol, M. Becquet, R. Hanus, Kinematic calibration and geometrical parameter identification for robots, Robot. Autom. IEEE Trans. 7 (1991) 721–732.
[17] B. Mooring The effect of joint axis misalignment on robot positioning accuracy, in: Proceedings of the Engineering Conference on ASME International Computers. 1983, pp. 151–156.
[18] W. Khalil, E. Dombre, Modeling, Identification and Control of Robots, Butterworth-Heinemann, Oxford, 2004.
[19] S. A. Hayati, Robot arm geometric link parameter estimation, in: Proceedings of the 22nd IEEE Conference on, Decision and Control 1983, pp. 1477–1483.
[20] H. Zhuang, Z.S. Roth, F. Hamano, A complete and parametrically continuous kinematic model for robot manipulators, Robot. Autom. IEEE Trans. 8 (1992) 451–463.
[21] M. A. Meggiolaro and S. Dubowsky, An analytical method to eliminate the redundant parameters in robot calibration, in: Proceedings of the IEEE International Conference on, Robotics and Automation ICRA'00 2000, pp. 3609–3615.
[22] M.R. Driels, W. Swayze, Automated partial pose measurement system for manipulator calibration experiments, Robot. Autom. IEEE Trans. 10 (1994) 430–440.
[23] Y. Bai, H. Zhuang, and Z. S. Roth, Experiment study of PUMA robot calibration using a laser tracking system, in: Proceedings of the IEEE International Workshop on Soft Computing in Industrial Applications SMCia/03. 2003, pp. 139–144.
[24] A. Rauf and J. Ryu, Fully autonomous calibration of parallel manipulators by imposing position constraint, in: Proceedings of the IEEE International Conference on, Robotics and Automation ICRA. 2001, pp. 2389–2394.
[25] S. Besnard and W. Khalil, Calibration of parallel robots using two inclinometers, in: Proceedings of the IEEE International Conference on, Robotics and Automation 1999, pp. 1758–1763.
[26] A. Rauf, A. Pervez, J. Ryu, Experimental results on kinematic calibration of parallel manipulators using a partial pose measurement device, Robot. IEEE Trans. 22 (2006) 379–384.
[27] A. Goswami, A. Quaid, and M. Peshkin, Complete parameter identification of a robot from partial pose information, in: Proceedings of the IEEE International Conference on, Robotics and Automation 1993, pp. 168–173.
[28] B.W. Mooring, Z.S. Roth, M.R. Driels, Fundamentals of Manipulator Calibration, Wiley, New York, 1991.
[29] C. Rao, H. Toutenburg, Linear Models and Generalizations: Least Squares and Alternatives, Springer, New York, 1999.
[30] H. Zhuang, J. Yan, O. Masory, Calibration of Stewart platforms and other parallel manipulators by minimizing inverse kinematic residuals, J. Robot. Syst. 15 (1998) 395–405.
[31] R. Fletcher, Practical Methods of optimization, John Wiley & Sons, Hoboken, NJ, Wiley, 2013 452 p.
[32] E. Moore, H., On the reciprocal of the general algebraic matrix, Bull. Am. Math. Soc. 26 (1920) 394–395.
[33] R. Penrose, A generalized inverse for matrices, Proc. Cambridge Philos. Soc (1955) 406–413.
[34] J.-H. Borm, C.-H. Meng, Determination of optimal measurement configurations for robot calibration based on observability measure, Int. J. Robot. Res. 10 (1991) 51–63.
[35] M.R. Driels, U.S. Pathre, Significance of observation strategy on the design of robot calibration experiments, J. Robot. Syst. 7 (1990) 197–223.
[36] H. Zhuang, O. Masory, and J. Yan, Kinematic calibration of a Stewart platform using pose measurements obtained by a single theodolite, in: Proceedings of the IEEE/RSJ International Conference on Intelligent Robots and Systems 95. Human Robot Interaction and Cooperative Robots 1995, pp. 329–334.
[37] M. A. Meggiolaro, G. Scriffignano, and S. Dubowsky, Manipulator calibration using a single endpoint contact constraint, in: Proceedings of ASME Design Engineering Technical Conference, Baltimore, USA, 2000.
[38] H. Zhuang, J. Wu, and W. Huang, Optimal planning of robot calibration experiments by genetic algorithms, in: Proceedings of the IEEE International Conference on, Robotics and Automation 1996, pp. 981–986.
[39] D. Daney, Y. Papegay, B. Madeline, Choosing measurement poses for robot calibration with the local convergence method and Tabu search, Int. J. Robot. Res. v24 (2005) 501–518.
[40] Y. Sun and J. M. Hollerbach, Observability index selection for robot calibration, in: Proceedings of the IEEE International Conference on, Robotics and Automation ICRA 2008, pp. 831–836.
[41] A. Nahvi and J. M. Hollerbach, The noise amplification index for optimal pose selection in robot calibration, in: Proceedings. of the IEEE International Conference on Robotics and Automation 1996, pp. 647–654.
[42] A. Nahvi, J. M. Hollerbach, and V. Hayward, Calibration of a parallel robot using multiple kinematic closed loops, in: Proceedings of the IEEE International Conference on Robotics and Automation 1994, pp. 407–412.
[43] D. Daney, Optimal measurement configurations for Gough platform calibration, in: Proceedings of the IEEE International Conference on, Robotics and Automation ICRA'02. 2002, pp. 147–152.
[44] H. Zhuang, K. Wang, and Z. S. Roth, Optimal selection of measurement configurations for robot calibration using simulated annealing, in: Proceedings of the IEEE International Conference on Robotics and Automation 1994, pp. 393–398.
[45] Y. Wu, Optimal pose selection for the identification of geometric and elastostatic parameters of machining robots, Ecole des Mines de Nantes, PhD Thesis (2014).
[46] Y. Chen, J. Gao, H. Deng, D. Zheng, X. Chen, R. Kelly, Spatial statistical analysis and compensation of machining errors for complex surfaces, Precis. Eng. 37 (2013) 203–212 1//.
[47] Z. Roth, B. Mooring, B. Ravani, An overview of robot calibration, Robot. Autom. IEEE J. 3 (1987) 377–385.
[48] H. Stone, A. Sanderson, and C. Neuman, Arm signature identification, in: Proceedings of the IEEE International Conference on, Robotics and Automation 1986, pp. 41–48.

[49] J. Denavit, R. Hartenberg, A kinematic notation for lower-pair mechanisms based on matrices, Trans. ASME J. Appl. Mech. 23 (1955) 215–221.
[50] K. Schröer, S.L. Albright, M. Grethlein, Complete, minimal and model-continuous kinematic models for robot calibration, Robot. Comput.-Integr. Manuf. 13 (1997) 73–85.
[51] A. Pashkevich, Computer-aided generation of complete irreducible models for robotic manipulators, in: Proceedings of the 3rd International Conference of Modellimg and Simulation. University of Technology of Troyes, France, 2001, pp. 293–298.
[52] H. Zhuang, F. Adviser-Hamano, and Z. S. Adviser-Roth, Kinematic modeling, identification and compensation of robot manipulators, PhD Dissertation, University Boca Raton, FL, USA, 1989.
[53] A. Klimchik, Y. Wu, S. Caro, B. Furet, A. Pashkevich, Geometric and elastostatic calibration of robotic manipulator using partial pose measurements, Adv. Robot. 28 (2014) 1419–1429.
[54] A. Klimchik, Y. Wu, G. Abba, S. Ganrnier, B. Furet, and A. Pashkevich, Robust algorithm for calibration of robotic manipulator model, in: Proceedings of the IFAC Conference on Manufacturing Modeling, Management and Control, Saint Petersburg, Russia, 2013, pp. 838–842.
[55] A. Klimchik, Y. Wu, A. Pashkevich, S. Caro, B. Furet, Optimal Selection of Measurement Configurations for Stiffness Model Calibration of Anthropomorphic Manipulators, Appl. Mech. Mater. 162 (2012) 161–170.
[56] A. Klimchik, S. Caro, A. Pashkevich, Optimal pose selection for calibration of planar anthropomorphic manipulators, Precis. Eng. 40 (2015) 214–229.
[57] A. Klimchik, A. Pashkevich, Y. Wu, B. Furet, S. Caro , In: C.-Y. Su, S. Rakheja, H. Liu (Ed.), Optimization of measurement configurations for geometrical calibration of industrial robot 2012. Intelligent Robotics and Applications, Springer, 132–143, http://dx.doi.org/10.1007/978-3-642-33509-9_13.
[58] S. Caro, C. Dumas, S. Garnier, and B. Furet, Workpiece placement optimization for machining operations with a KUKA KR270-2 robot, in: Proceedings of the IEEE International Conference on Robotics and Automation (ICRA). 2013, pp. 2921–2926.
[59] C. Dumas, S. Caro, M. Cherif, S. Garnier, B. Furet, X. Zha, et al., Joint stiffness identification of industrial serial robots, Robotica 30 (2012) 649–659.
[60] Kuka, ⟨http://www.kuka-robotics.com⟩.
[61] Leica-geosystems. ⟨http://metrology.leica-geosystems.com/en/index.htm⟩.